We are IntechOpen, the world's leading publisher of Open Access books Built by scientists, for scientists

4,800
Open access books available

122,000
International authors and editors

135M
Downloads

Our authors are among the

154
Countries delivered to

TOP 1%
most cited scientists

12.2%
Contributors from top 500 universities

CLARIVATE ANALYTICS BOOK CITATION INDEX INDEXED

WEB OF SCIENCE™

Selection of our books indexed in the Book Citation Index in Web of Science™ Core Collection (BKCI)

Interested in publishing with us?
Contact book.department@intechopen.com

Numbers displayed above are based on latest data collected.
For more information visit www.intechopen.com

2

Gas-Liquid Two-Phase Flow Rate Measurements by Flow Division and Separation Method

Dong Wang
XI'an Jiaotong University
People's Republic of China

1. Introduction

In this chapter we shall introduce a new and practical method for two-phase flow rate measurement, which is known as flow division and separation method. As its name suggested, a two-phase flow is measured by diverting a small fraction of the total stream to a division loop and metering it with the separation means. This method has been developed in Xi'an jiaotong university since the end of last century, and extensively studied in laboratory, some of the meters have been successfully applied in engineering. At first we briefly introduce the flow division technique in single phase flow, then we discuss how this method can be used in gas-liquid two-phase flow measurements, further more we shall give three detail examples of this kind of two-phase flow meters.

2. Flow measurement by flow division technique

The rate of flow in a pipe can be measured by a flowmeter installed in the identical pipe, this kind of flowmeter is called the full bore flowmeter which has the same size of diameter as the flow tube. However as the flow tube becomes very large, the full bore flowmeter will be extremely expensive or even impossible to build. In this case, the flow division technique can be a very convenient choice. In addition to this, the flow division technique can also be used to solve the difficult problem of two-phase flow measurement.

2.1 Flow division technique in single phase flow

Flow division technique, also called flow ratio technique (DeCarlo, 1984), have been widely used in single phase flow measurements, whose main feature is to use a small size meter to measure a large volume flow in large lines. This kind of flow meter is usually called "bypass flow meter", or "shunt flow meter" or "proportional flow meter". As shown in Fig.1, a bypass flow meter consists of three major portions (Fenelon,1994), a main flow path, a bypass loop (flow division branch) and a restriction. The restrictive element is positioned in the main flow path and the bypass flow loop is arranged to cross the restrictive element, so that its inlet and outlet is located at the upstream and downstream of the restrictive element respectively. The function of the restrictive element is to create a pressure drop between the

upstream and downstream of the restriction which will cause a portion of total flow to enter into the bypass loop. A small size flow meter is installed in the bypass flow loop to meter the flow quantity or flow rate passing through the bypass loop. The total flow quantity or flow rate can be inferred from the metered value since a definite ratio exists between the flow rate in bypass loop and the total flow rate.

From Fig.1 we can also see that the bypass loop and the main flow path have a common inlet and a common outlet i.e. they are in parallel to each other (Munson, 2002). In accordance with the nature of parallel loops, the pressure loss of these two loops must be equal (Munson,2002). The pressure loss in these two loops include friction and local resistance which can be express as

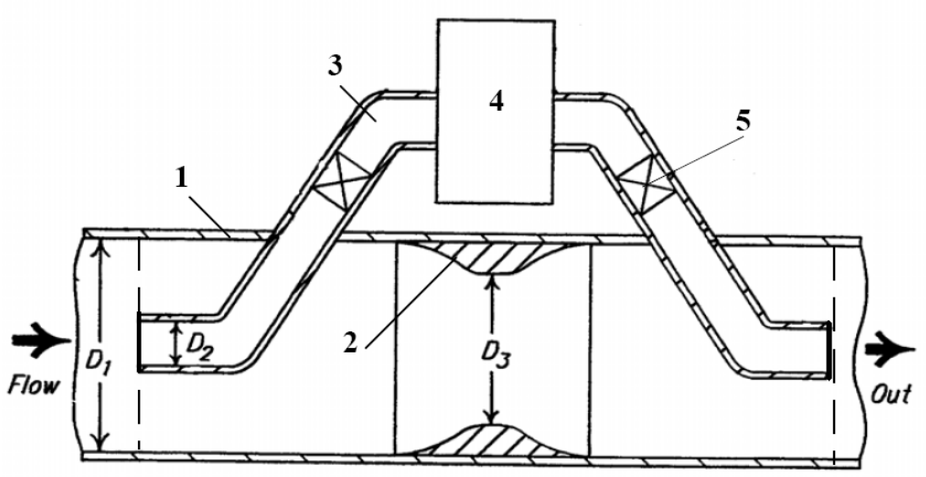

1. Main flow path; 2. Restrictive element; 3. Bypass loop; 4. Flow meter; 5. Valve

Fig. 1. Schematic represent of a bypass flow meter

$$\Delta P_2 = \left[\sum \lambda_2 \frac{l_2}{D_2} + \sum \xi_2 \right] \frac{1}{2\rho} \left(\frac{M_2}{A_2} \right)^2 \tag{1}$$

$$\Delta P_3 = \left[\sum \lambda_3 \frac{l_3}{D_3} + \sum \xi_3 \right] \frac{1}{2\rho} \left(\frac{M_3}{A_3} \right)^2 \tag{2}$$

Where Δ P is the pressure loss, λ is Darcy friction factor, l is tube length, D is tube inner diameter, ξ is local loss factor, ρ is the density of fluid, M is mass flowrate, A is tube cross section area, Symbol Σ represents summation; Subscript "2" represents the main flow path and the subscript "3" represents the bypass loop. Since $\Delta P_2 = \Delta P_3$, we can obtain the ratio of M_2 to M_3 from equation (1) and (2)

$$\frac{M_2}{M_3} = \frac{A_2}{A_3} \sqrt{\frac{\sum \lambda_3 \frac{l_3}{D_3} + \sum \xi_3}{\sum \lambda_2 \frac{l_2}{D_2} + \sum \xi_2}} \tag{3}$$

As the total flow rate M_1 equals to the sum of M_2 and M_3, therefore the ratio of M_3 to M_1 can be derived from equation (3)

$$\frac{M_3}{M_1} = \frac{1}{1 + \frac{A_2}{A_3}\sqrt{\frac{\sum \lambda_3 \frac{l_3}{D_3} + \sum \xi_3}{\sum \lambda_2 \frac{l_2}{D_2} + \sum \xi_2}}} \tag{4}$$

Equation (4) clearly shows that the ratio of flow rate passing through the bypass loop to the total flow is dependent on the structure parameters of these two loops. By properly setting the resistance devices in these two loops, a constant ratio can be obtained. In practice the ratio should be calibrated by experiment, and a bypass flow meter will have an equivalent precision as the full bore meter.

The ratio of M_3 to M_1 can vary from 1 to 2.5×10^{-4}, hence the flow meter in the bypass loop can be greatly reduced in size. We can use a small size flow meter or flow sensor to meter a large volume flow in a large pipe. Thus the capital cost and operation cost can be significantly reduced. This is the main advantage of a bypass flow meter.

The flow meter incorporated in bypass loop can be a flow quantity meter for measuring the quantity of flow (Hirst, 1951; Hodgson,1932; Kidder, 1934; Peranio, 1967;Thomson, 1895a, 1895b), or a flow rate meter for measuring the rate of flow.

The flow rate meters used in the bypass loop can be any types, but we usually select the meters which have a relative large metering range, for example, it can be a rotameter (Rlkuta,1969; Stenberg,1962), a Coriolis mass flow meter (Kane, 1994; Kalotay,1994;Van Cleve,1999), or a thermal (calorimetric) mass flowmeter (Adams,1969; Baker,1969, 1971,1977; Hawk,1984;Kronberger,1952; Laub,1956; Sato,1983). Therefore a bypass flow meter will also have a large metering range. At the same time, the flow meter or a flow sensor will also have a higher sensitivity than the full bore flow meter because of its small size. For instance, a small size Coriolis effect flow sensor is more sensitive than a large one because of its thinner and more flexible flow tube which is more suitable for the generation of meaningful Coriolis forces (Kalotay,1994).

A bypass flow meter's metering range and precision can be further expanded and improved if a variable constriction is used. Fig.2 is an example of variable constriction flow meter (Bahrton,1996). The significant feature of the variable constriction in Fig.2 is that a moveable conical body is introduced in the orifice. When the total flow is very low, the conical body will be pressed to the left by the spring so as to decrease the flow area of the orifice or completely close the orifice, so that all of the flow, or at least a large part of the total flow will enter into the bypass loop and metered by the flowmeter. On the contrary, when the flow is large, the conical body will be forced to the right by the fluid so as to increase the flow area of the orifice, so that a smaller part of total flow will pass through the bypass loop. As a result the dynamics (the ratio of maximum flow rate to the minimum flow rate) of the bypass meter can be expanded to 2500:1 which is much larger than a full bore flow meter. It can also be seen from Fig.2 that in any case the flow passing through the bypass loop can always fall in the optimum measuring arrange of the flow meter by adjusting the restriction,

and this will improve the precision of the flow meter. Similar structure can also be found in references (Connet,1928; Olin,1984).

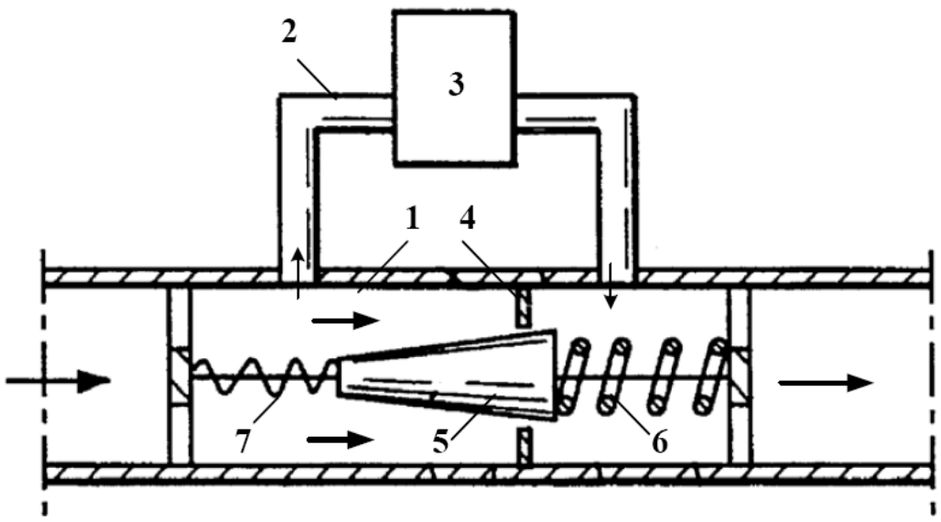

1. Main flow path; 2. Bypass loop; 3. Flowmeter; 4. Orifice plate; 5.Connical body; 6,7. Spring

Fig. 2. Bypass flowmeter with a variable constriction

The restrictive element in a bypass flow meter can be also a Venturi tube (Van Cleve,1999), a nozzle(Baker,1971), a pitot tube (Baker,1977) or other resistance devices.

2.2 Recent development in two-phase flow measurement

Two-phase flow rate measurement is still a difficult problem in science and engineering. Traditional solution is to separate the two-phase mixture into single phase flows first, and then measure the flow rate of each phase with single-phase flow meters. In this method, usually a large separator vessel is required to complete the separation of two-phase flow, and both the capital and operating cost of equipments tend to be high. Also, in practice, the measurements derived from this process are subject to many errors（Thorn et al ,1997）. During the last couple of decades, a number of techniques have been studied to measure the two-phase flow rate. Nearly all the conventional flow meters have been tried to meter the two-phase flow(Bates and Ayob ,1995; Cha et al ,2002; Chisholm ,1974; Jung et al ,2009; Kriiger et al,1996; Lin,1982; Murdock,1962; Skea and Hall,1999; Steven,2002; Steven and Hall,2009). Experiments show that the measurement errors will increase rapidly as the amount of second phase appeared in the flow increases. At the same time, the response of a single phase flowmeter to the two-phase flow depends on not only the flowrate but also on the phase fraction. For instance, under a certain flowrate, the higher the gas quality, the larger the differential pressure passing through an orifice. Therefore, a single phase flowmeter is not capable of measuring the flowrate and phase fraction simultaneously and a combination with other measuring devices is necessary. A lot of combined methods have been developed to measure the two-phase flowrate and phase fraction (Huang et al ,2005; Geng et al ,2007; Meng et al ,2010; Meribout et al ,2010; Oliveira et al ,2009; Reis and Jr ,2008; Sun ,2010; Zhang et al ,2010; Zheng et al ,2008).

These combined methods mentioned above can work well within their respective metering ranges, however, the measurement error would increase and the instruments may even fail to work once beyond their narrow rated ranges. One of the major reasons that cause the larger measuring error and the failure of measurement is that a two-phase flow is always in violent fluctuation. Fluctuation is an inherent feature of two-phase flow that makes the instruments unsteady and unreliable. Nevertheless some researchers consider it as useful information to determine the phase fraction or flowrate of a two-phase flow (Beg and Toral ,1993; Ferreira ,1997; Wang and Tong ,1995; Xu et al ,2003). A separation means for two-phase flow measurement that does not employ large separator may be a good choice (Liou ,1995; Turkowski ,2004).

2.3 Two-phase flow measurement by flow division and separation method

From section 2.1 it has been known that the flow division technique is a reliable method for measuring the single phase flow rate. Its main advantage is to use a small size meter to measure the total flow in a large flow pipe. If this method can be used in gas-liquid two-phase flow, then we can use a small size separator in the bypass loop to separate the two-phase mixture passing through the bypass loop into single phase gas and liquid and consequently measuring them by conventional single phase flowmeters, thus the problem of two-phase flow rate measurement can simply be solved. However, there is a key problem which must be solved before this technique can be successfully used in two-phase flow, that is how to divert a portion of two-phase mixture, which will have the same components as the total flow and be proportional to the total flow, to the bypass loop. We can not simply place the inlet end opening of the bypass loop in the main flow as in the case of single phase flow, because a two-phase fluid is not a homogenous medium, on the contrary, it always presents different flow pattern at different flow conditions. Hence a special distributor must be employed between the main and bypass loop. Fig.3 shows a schematic representation of a flow division type two-phase flow measurement system (Wang & Lin, 2002). The measuring process is that, first, a small portion (1%—20%) of the total two-phase flow is extracted by a distributor, then it is separated by a small compact separator, after that the separated gas and liquid flows are metered by the single phase flowmeter respectively, in the end, the two metered flows are returned to the main stream. The total gas flow rate M_G and total liquid flow rate M_L are determined by the following equations

$$M_G = \frac{M_{G3}}{K_G} \tag{5}$$

$$M_L = \frac{M_{L3}}{K_L} \tag{6}$$

Where M_{G3} and M_{L3} is the metered gas and liquid flow rate respectively, K_G and K_L represents the gas and liquid extraction ratio respectively. For an ideal distributor, K_G and K_L should be a constant so that the determinations of total flow rate of each phase would be much simpler. Apparently, it is difficult for a real distributor to keep the extraction ratio being constant in any condition. In fact, as long as K_G and K_L could be relatively stable within a quite wide range, the distributor could be used. From Fig.3 it can also been seen that the flow rate of the stream entering into the separator is only 1%—20% of the total

flow, so the size of separator can be reduced at least 1%—20% times compared with the traditional separating method in which all the two-phase mixture is separated, and the size of a two-phase flow meter may nearly approach that of common single flow meter. In the following section we shall introduce three different distributors.

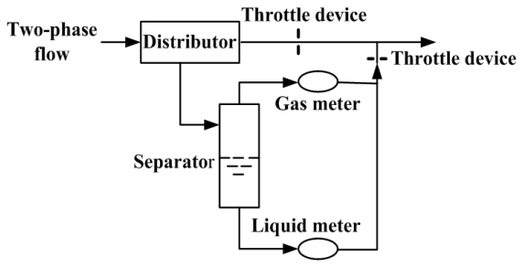

Fig. 3. Schematic representation of a flow division type two-phase flow measurement system

2.3.1 Rotation drum distributor

Fig. 4 shows the schematic drawing of the drum distributor (Wang & Lin, 2002). The core part of a rotational drum distributor is the rotational drum. The outline of the drum is a cylinder, the inside space is equally segregated into a series of small flow channels which twisted around the drum axis. The outputs of the most channels are directed to the down stream part of the pipe, only a few channels, which are selected as the extraction channels, are connected to the separator (to the bypass loop).

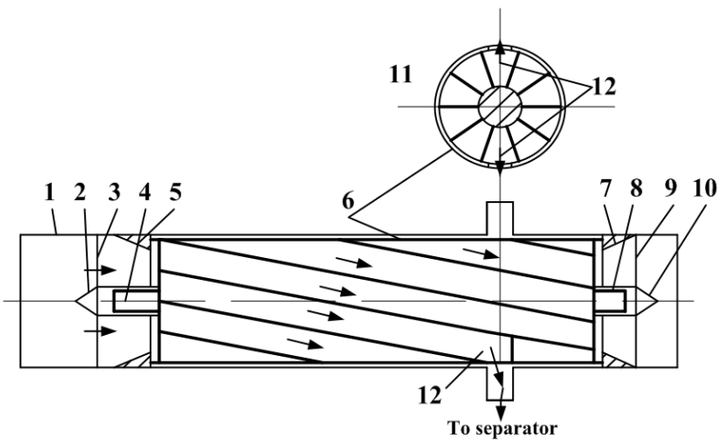

1. Shell; 2,10. Bearing seat; 3,9. Bracket; 4,8. Shaft; 5. Front guide cone; 6. Rotation drum; 7. Back guide cone; 11. Normal channel; 12. Extraction channel.

Fig. 4. Schematic drawing of a rotational drum distributor

As two-phase mixture passes through channels, the drum will be forced to run at a high speed around its axis by the fluid. With the running of the drum, the entrance of each channel will continuously scan over every point on the cross section in front of the drum. If each channel has the same characteristics of geometry, friction and output pressure, and the rotation speed is high enough, then the flow of fluid at any point on the cross section in

front of the drum would not be influenced by the rotating of the rotational drum, and would have the same possibility to enter each channel. In other words, the flow would be considered as steady flow within a drum running period and the time duration Δt, during which the fluid at any point of the cross section in front of the drum flowing into a channel within a drum rotation period, will be equal, that is

$$\Delta t = \frac{T}{n} \tag{7}$$

Where T is the drum rotation period; n is the total number of the channels inside the drum.

The amount of gas and liquid passing through each channel in a drum rotation period will be

$$\Delta M_G = \int_A \Delta t \alpha_i u_{Gi} \rho_G dA = \Delta t \rho_G \int_A \alpha_i u_{Gi} dA = \Delta t M_G \tag{8}$$

$$\Delta M_L = \int_A \Delta t (1-\alpha_i) u_{Li} \rho_L dA = \Delta t \rho_L \int_A (1-\alpha_i) u_{Li} dA = \Delta t M_L \tag{9}$$

Where ΔM_G and ΔM_L is the amount of gas and liquid passing through each channel in a drum rotation period respectively; α_i is the local void fraction and u_{Gi}, u_{Li} is the local gas and liquid velocity on the cross section in front of the drum respectively; ρ_G and ρ_L is the gas and liquid density respectively; A represents the cross section of the pipe in front of the drum. M_G and M_L is the total gas and liquid flow rate respectively.

Equation (8) and (9) also mean that ΔM_G and ΔM_L is equal to the amount of total flow of each phase passing through the cross section of the pipe in front of the drum within time Δt respectively. The drum distributor seemingly acts as a time controlled switch which equally directs the total flow into each channel. As long as the rotation period of drum is short enough, the accuracy of Equation (8) and (9) will be all right.

The average gas flow rate m_G, and liquid flow rate m_L passing through each channel will be

$$m_G = \frac{\Delta M_G}{T} = \frac{\Delta t}{T} M_G = \frac{M_G}{n} \tag{10}$$

$$m_L = \frac{\Delta M_L}{T} = \frac{\Delta t}{T} M_L = \frac{M_L}{n} \tag{11}$$

If z channels are selected as the extraction channels, which are connected to the separator, then the sum of gas flow rate M_{G3} and liquid flow rate M_{L3} of the bypass stream is

$$M_{G3} = \frac{z}{n} M_G \tag{12}$$

$$M_{L3} = \frac{z}{n} M_L \tag{13}$$

The gas extraction ratio K_G, and liquid extraction K_L is

$$K_G = \frac{M_{G3}}{M_G} = \frac{z/n M_G}{M_G} = \frac{z}{n} \tag{14}$$

$$K_L = \frac{M_{L3}}{M_L} = \frac{z/n M_L}{M_L} = \frac{z}{n} \tag{15}$$

Equation (14) and (15) show that the extraction ratio of the rotational drum distributor is simply dependent upon the number of extraction channels and independent of the flow patterns. In the experiment of this study, n, the total number of channels, is 10, z, the number of extraction channels, is 2. According to Equation (14) and (15), the extraction ratio should be

$$K_G = K_L = \frac{2}{10} = 0.2 \tag{16}$$

Equation (14) – (16) are obtained for a perfect rotational drum distributor. There are some factors which should be considered when use them to a real rotational drum distributor. These include the size of the gap between the drum and the shell, the rotating speed of the drum and the geometrical departure from the ideal shape during the manufacturing and the assembling process. All these effects on the extraction ratio will be determined by experiments.

Two different drums were used in the experiments in order to examine the effect of gap size between the shell and the drum on the extraction ratio. One drum has 0.75 mm gap size, and another one has 0.25 mm gap size. The experiments were carried out in an air-water two-phase flow loop in Xi'an Jiaotong University as shown in Fig.5.

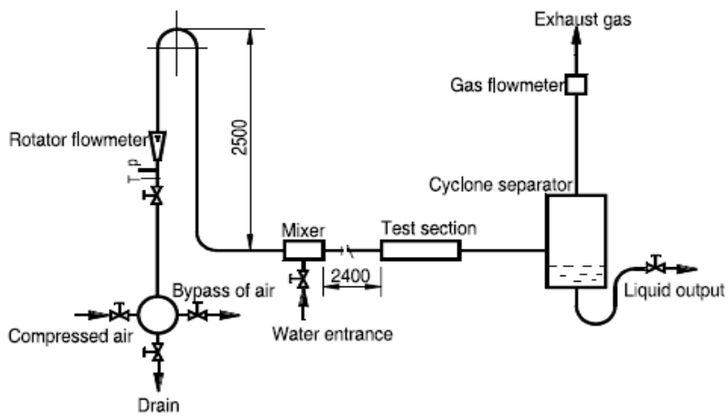

Fig. 5. The air-water two-phase flow experimental loop schematic

A gas rotameter was installed vertically upstream of the mixer for air flow rate adjustment, the precise gas flow rate was given by the vortex flow meter installed at the top of cyclone separator at the outlet end of the loop. The gas flow rate of the extracted (bypass) stream was also metered by a vortex flow meter. The water flow rates, both the total water flow rate and the extracted (bypass) water flow rate, were metered at the point of liquid output in the water leg of the cyclone separator and of the separator used in the bypass loop respectively

by using the weight—time method. The duration of time during which water is collected was about 10 – 120 s, depending upon the flow rate of the water. An assessment was carried out on the uncertainty on each of the measured parameters. They were all within ±1.5%. From this the accuracy of the extraction ratio was determined and found to be ±1.5% for liquid extraction ratio K_L, and ±2% for gas extraction ratio K_G. The separator used in the bypass loop in this experiment was simply a vertically installed cylinder made from Plexiglas pipe, mounted internally with a multi-hole plate in the cross section of the cylinder just above the entrance of the bypass stream. The inner diameter and height of the separator were 70 and 350 mm respectively. The straight pipe between the mixer and the test section has 30 mm ID and 2400 mm total length, and is made from Plexiglas pipe through which the flow patterns can be observed.

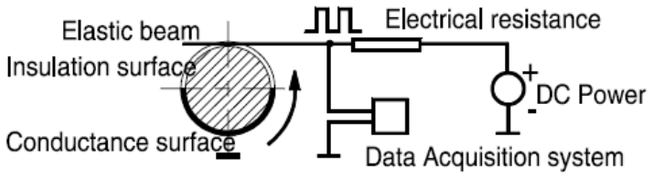

Fig. 6. The rotation speed measuring circuit

In order to determine the effect of rotation speed of the drum on extraction ratio, a simple electrical circuit as shown in Fig. 6 was used to measure the rotation speed of the rotational drum. A short portion (about 3 mm wide) of the drum shaft was selected as one part of the circuit. Half of the outer surface of the shaft was coated with a thin layer of plastic to form the insulation surface, and the other half was a polished metal surface. An elastic beam made from thin copper – beryllium plate, is contacted to the shaft at one end, and is connected to the electrical resistance at the other end. With the running of the shaft, the elastic beam contacts alternatively with insulation surface and conductance surface. Thus, a square electric current pause is generated in the circuit for each cycle. The square wave signal can be seen on the screen of the data acquisition system, and the frequency of the square wave represents the drum rotation speed. If some water is appeared on the insulation surface, the amplitude of square wave signal will be reduced a little, but the shape and frequency of the square wave will not be changed any more, even the pipe is full of water.

Extraction ratio were measured in the following experiment range: gas superficial velocity varied between 4 and 40 m/s; water superficial velocity ranged from 0 to 0.28 m/s; flow patterns occurring during experiments included stratified flow, wave flow and annular flow. A typical experimental results of the extraction ratio are shown in Fig. 7, data symbol S, W and A represents the flow pattern of stratified, wave and annular flow respectively. These results were obtained with the drum having 0.25 mm gap size between the shell and the drum. From these results it is seen that both the gas extraction ratio and liquid extraction ratio are very close to the theoretical value—0.2 as the extracted (bypass) liquid flow rate is high, but as the extracted liquid flow rate is low, the liquid extraction ratio becomes higher than 0.2, while the gas extraction ratio becomes lower than 0.2. For the liquid extraction ratio, this phenomena could be explained by the fact that some of the liquid will preferentially leak into the separator through the gap between the shell and the drum, rather

than through the flow channels in drum as two-phase flow passing through the distributor. Therefore the actual liquid flow rates extracted are a little more than the theoretical values (predicted with Eq. (13)). This liquid leakage is generally quite small compared to the total liquid flow rate extracted when the liquid flow rate is high, so the extraction ratio is close to 0.2; but when the liquid flow rate is low, the liquid leakage will not be a small value compared to the total liquid flow rate, and the liquid extraction ratio K_L will be much higher than 0.2. The larger the gap is, the more apparent this tendency will be, as shown in Fig. 8, which was obtained with the drum having 0.75 mm gap size. Thus if the leakage could be effectively controlled by reducing the gap size between the drum and shell as far as possible or by other means, the stability of K_L would be improved significantly.

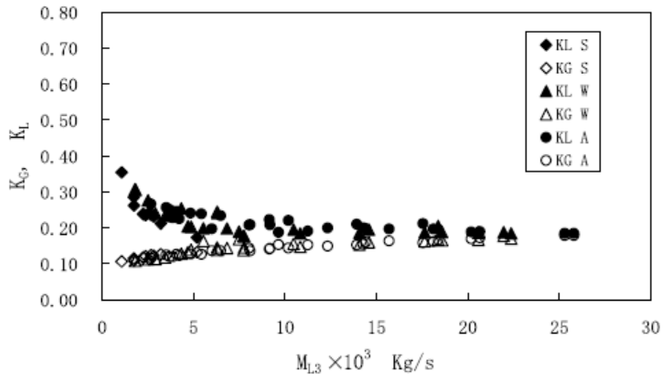

Fig. 7. Experimental result of extraction ratios (0.25 mm gap size)

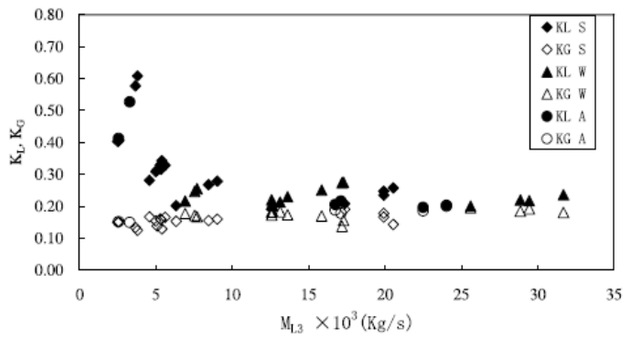

Fig. 8. Experimental result of extraction ratios (0.75 mm gap size)

For the gas extraction ratio K_G, the explanation is that the resistance to the air flow in the main flow loop is low compared to the bypass loop as the liquid flow rate is low, so some gas that should flow into the bypass loop will remain in the main loop, and the extraction ratio will be lower than 0.2; with the increase of the liquid flow rate, the resistance to the air flow in the main flow loop will increase, this make more gas flow into the bypass loop, and the gas extraction ratio increases gradually. Since the total resistance in main loop (and also bypass loop) comprises two parts: the resistances in drum and after the drum, it is easy to balance the first part of total resistance in main loop with that in bypass loop (as every flow channel of the drum nearly has the same geometry), and yet it is not easy to balance the second part in main loop with that in bypass loop, so it is the unbalance of the second part

of total resistance in main loop and in bypass loop that causes the variation of K_G. If the second part of total resistance in both loops could be restricted within a very small fraction compared to the first part (or total resistance), the variation of K_G would be reduced remarkably. From Fig. 7 and Fig. 8 it can also be seen that flow regime do not have significant effect on the extraction ratios in the experimental range. The effect of rotation speed of the drum on the extraction ratio is shown in Fig.9, where V_{SL} represents superficial liquid velocity in the straight pipe. These data were obtained at arbitrary liquid and gas flow rates which cover the range of experiment. Although significant variations of extraction ratios can be seen in Fig. 9, any definite relationship between the variations and rotation speed of the drum can't be seen except the data of K_L at low liquid superficial velocity V_{SL} < 0.028 m/s. The extraction ratios, K_G and K_L, are only dependent upon the superficial liquid velocity. At the same nominal superficial liquid velocity, K_G (or K_L) is nearly unchanged over the span of rotation speed. All the higher value points of K_L and lower value points of K_G occur at the condition of low superficial liquid velocity V_{SL} < 0.028 m/s, the reason for this has been explained above. The value of K_L at low superficial liquid velocity V_{SL} < 0.028 m/s increases with increasing rotation speed, this can be further explained by the fact that the drum is driven by the fluid to be measured, so the rotation speed is nearly proportional to the gas flow rate at low superficial liquid velocity. Therefore, the increase in rotation speed means the increase in gas flow rate that will cause a higher pressure difference between the inlet and exit of the drum distributor, and of course a higher liquid leakage through the gap between the shell and the drum and finally a higher value of K_L. It is the gas flow rate that affects the value of K_L at low superficial liquid velocity. The rotation speed of drum does not have significant effect on the extraction ratios in the experimental range.

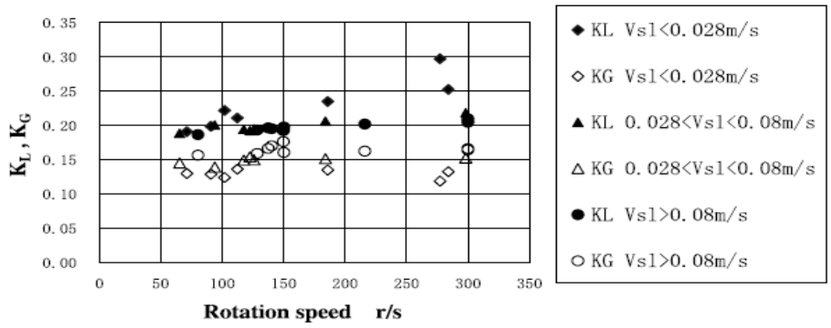

Fig. 9. Effect of rotation speed on extraction ratios (0.25 mm gap size)

Figs. 7 and 8 can also be considered as the extraction ratio calibration curves. By using these calibration values of K_G and K_L, the total gas flow rate and liquid flow rate can be determined according to Equation (5) and (6) respectively. The average error of flow rate measurement in the experiments were about ±6.2% and ±5.1% for gas and liquid respectively when the drum gap size was 0.75 mm; and ±5.6%, ±3.4% when the drum gap size was 0.25 mm.

2.3.2 The wheel – Fluid rooms distributor

Two type of wheel—fluid rooms distributors are schematically shown in Fig.10 and Fig.11 respectively (Wang et al, 2012).

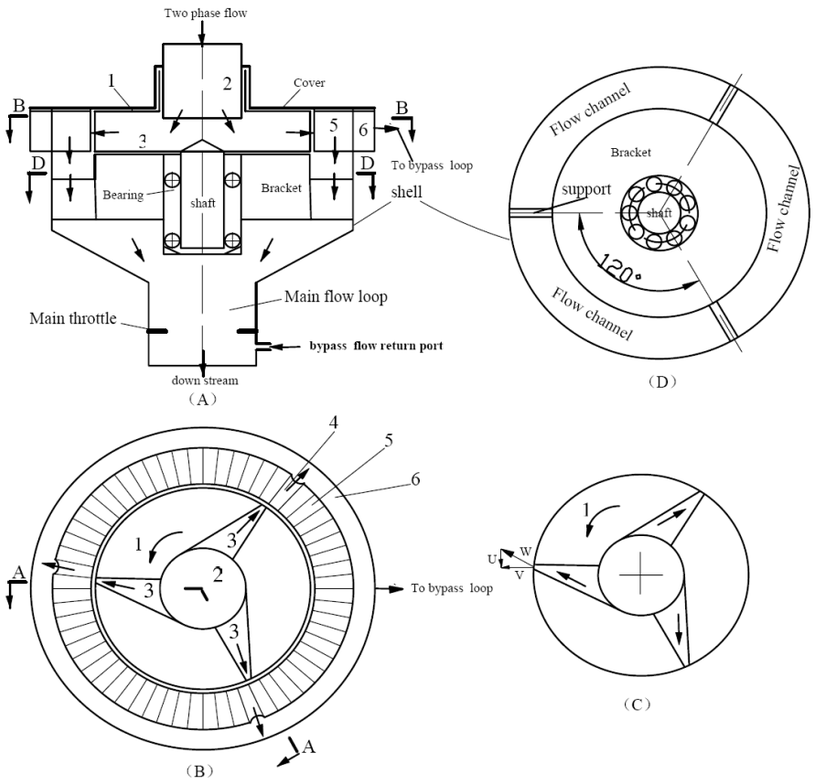

1.Wheel; 2.Entrance of flow; 3.Flow path; 4.Bypass fluid room; 5.Main fluid room; 6.Header of bypass flow

A. Rotated sectional view A-A; B. Sectional view B-B; C. Velocity triangle; D. Sectional view D-D

Fig. 10. The wheel—fluid rooms distributor-passive type

From Fig.10 it can be seen that the main body of the distributor consists of two parts: a wheel and a number of fluid rooms (Fig.10B). The wheel is located at the center of the distributor, and the fluid rooms equally surround the wheel. These fluid rooms are divided into two groups, one is connected to the main flow loop through their bottom (Fig. 10A), which is named as main fluid rooms; the other is connected to the bypass loop through the header of bypass flow (Fig.10B,A), which is called bypass fluid rooms. In Fig.10 the number of bypass fluid rooms is 3 and they are arranged 120 degrees from one to another around the wheel (Fig. 10B). As shown in Fig. 10A, the wheel is vertically installed in the bracket with a shaft and two bearings. The planform of bracket is shown in Fig. 10D. The wheel can rotate about its center axis, and is flow driven. In Fig.10A, the cover of distributor is made from Plexiglas plate for an easy observation of the wheel rotation. The fluid entrance of the distributor is located at the center of the cover, from where a short tube, which is fixed into the cover is inserted into the wheel center. There are 3 flow paths that equally surround flow entrance extending to the edge of the wheel (Fig.10B). As two-phase mixture flow downwards into the center of wheel (Fig.10A), the fluids will pass through the 3 flow paths within the wheel (Fig. 10B) and form 3 jets at the exit of the path. A reaction force will act on the wheel when the jets leave, which has a component in the tangency direction of wheel and push the wheel to rotate around the shaft at a high speed. The velocity triangle of the jets is shown in Fig.10C, where w is the relative velocity of the fluids, U is the wheel linear

velocity at the edge, and V is the absolute velocity of fluids. It can be seen that V is nearly in the radial direction of the wheel, which means that the fluids can flow directly into the fluid rooms without impacting with the side wall of fluid rooms, and this will reduce the pressure loss of the distributor. With the rotation of wheel, the total two-phase flow is conducted alternately into main flow loop and bypass loop through their corresponding fluid rooms.

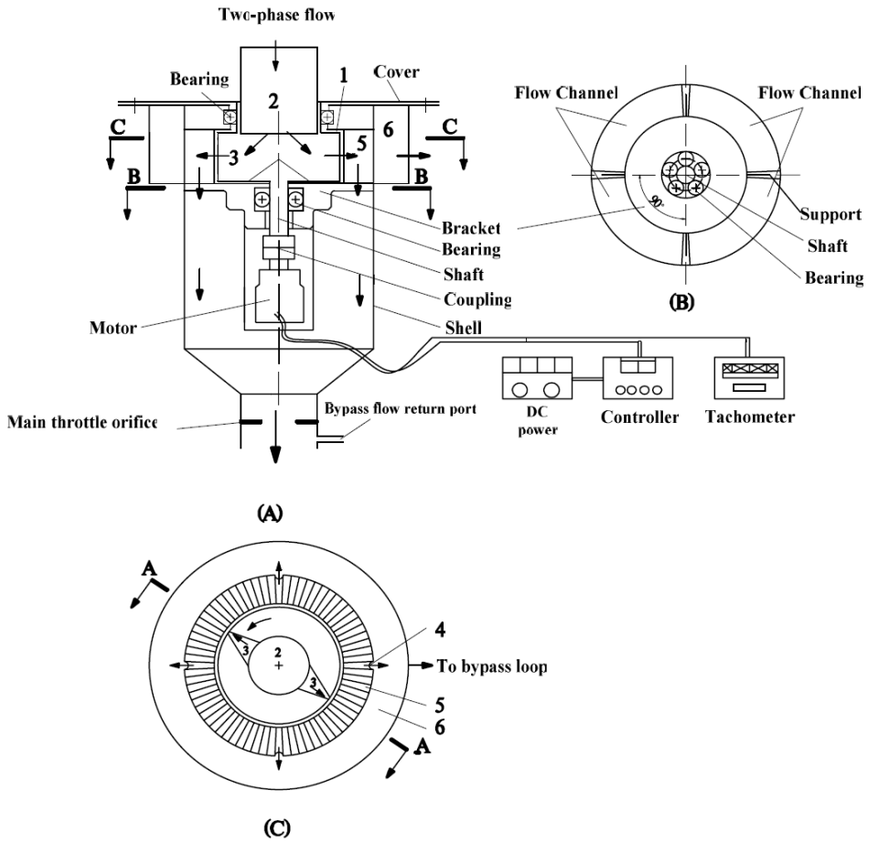

1.Wheel; 2.Entrance of flow; 3.Flow path; 4.Bypass fluid room; 5.Main fluid room; 6.Header of bypass flow

A. Rotated sectional view A-A; B. Sectional view B-B; C. Sectional view C-C

Fig. 11. The wheel—fluid rooms distributor-active type

Fig.11 is similar to Fig.10, only the wheel is driven by a motor and the rotation speed of the wheel is controlled by adjusting the electrical current to the motor. There are totally 4 bypass fluid rooms arranging 90 degrees from one to another around the wheel (Fig.11C). The number of flow paths within the wheel is 2 (Fig.11C). This distributor is designed for low velocity condition when the fluid can not drive the wheel steadily.

To be similar to a rotational drum, the wheel can evenly distributes the total flow to each fluid room during rotation, hence the relationship between M_{1j} and M_{3j} (where M is flowrate, j represents an arbitrary phase, gas or liquid, 1 presents total flow and 3 is the bypass flow) in the distributor mentioned above can be obtained based on the mass conservation within one period of rotation of the wheel. The amount of an arbitrary phase flowing to the bypass loop is

$$\Delta m_j = m \times \frac{T \times M_{1j}}{n} = T \times M_{3j} \tag{17}$$

where n is the total number of the fluid rooms, which is equal to 60 in Fig.10 and 72 in Fig.11; m is the number of bypass fluid rooms, which is 3 in Fig.10 and 4 in Fig.11 respectively; T represents the rotation period of the wheel.

Rearranging Equation (17), the extraction ratio will become

$$K_j = \frac{M_{3j}}{M_{1j}} = \frac{m}{n} \tag{18}$$

Equation (18) shows that the extraction ratio depends only on the ratio of bypass fluid room number to the total fluid room number and is independent of the speed of rotation. The rotation period changes with the flow rate, while the extraction ratio will still remain constant. We can change the value of the extraction ratio by altering the value of m or n. In the present study, for the passive distributor of Fig.10, m=3, n=60, according to Equation (18), the theoretical value of extraction ratio K_j is 0.05; and m=4, n=72 ,K_j=0.0556 for the active distributor of Fig.11. It should be pointed out that Equation (17)—(18) are only correct under the isokinetic sampling condition, i.e. the flow to each fluid room (refer to Fig.10B or Fig.11C) must be equal (let it equal to q), hence the bypass flow rate should equal to mq, the main flow rate be (n-m)q and the total flow rate be nq. In order to meet this requirement, the resistance in bypass flow loop and main flow loop must be properly controlled. The pressure loss due to friction and local resistance in these two loops can be written as below based on homogeneous flow model (Butterworth et al, 1978)

$$\Delta P_3 = \left[\sum \psi_3 \lambda_3 \frac{l_3}{D_3} + \sum \xi_3 \right] \frac{1}{2\rho_L} \left(\frac{M_3}{A_3} \right)^2 \left[1 + X_3 \left(\frac{\rho_L}{\rho_G} - 1 \right) \right] \tag{19}$$

$$\Delta P_2 = \left[\sum \psi_2 \lambda_2 \frac{l_2}{D_2} + \sum \xi_2 \right] \frac{1}{2\rho_L} \left(\frac{M_2}{A_2} \right)^2 \left[1 + X_2 \left(\frac{\rho_L}{\rho_G} - 1 \right) \right] \tag{20}$$

Where △P is the pressure loss, Ψ is correction factor, λ is Darcy friction factor, l is tube length, D is tube inner diameter, ξ is local two phase flow loss factor, ρ_L is the density of liquid phase, ρ_G is the density of gas phase, M is mass flowrate, A is tube cross section area, and X is the gas quality; Symbol Σ represents summation; Subscript "2" represents the main flow loop and the subscript "3" represents the bypass flow loop. Although Equation (19) and (20) are derived from the homogeneous flow model, they have been corrected by experimental data and several correlations about Ψ and ξ have been established for engineering application, especially in China and Russia (Lin et al, 2003).

From Fig.3 it can be seen that the bypass flow loop and the main flow loop have a common inlet and a common outlet i.e. they are in parallel to each other (Munson 2002), in accordance with the nature of parallel loops, the pressure loss of these two loops must be equal (Munson 2002). In isokinetic sampling case, $X_2 = X_3 = X_1$, where X_1 is gas quality of total flow, and the fluid densities are also equal. If we neglect the possible small difference of static head between two loops, the left hand sides of Equation (19) and (20) are equal. From

Equation (18), (19) and (20), a relationship of resistances between two loops for isokinetic sampling can be obtained

$$\frac{1}{1+\frac{A_2}{A_3}\sqrt{\frac{\sum\psi_3\lambda_3\frac{l_3}{D_3}+\sum\xi_3}{\sum\psi_2\lambda_2\frac{l_2}{D_2}+\sum\xi_2}}}=\frac{M_3}{M_3+M_2}=K \tag{21}$$

Where M_3 is the mass flowrate of bypass flow, and M_2 is the mass flow flowrate of main flow. This means that the resistance in two loops should be adjusted according to Equation (21) once an expected extraction ratio is selected. To make this work become easier, a main throttle device and a smaller throttle device are installed in main loop and bypass loop respectively. These two devices produce the major pressure loss in the corresponding loop, and Equation (21) can be met by merely adjusting these two throttle devices. In this case the pressure loss due to friction and other local resistances can be neglected, Equation (21) can be simplified as

$$\frac{1}{1+\frac{A_2}{A_3}\sqrt{\frac{\xi_3}{\xi_2}}}=\frac{M_3}{M_3+M_2}=K \tag{22}$$

Where ξ_3 and ξ_2 are the two-phase resistance factors of throttle devices in the bypass loop and main loop respectively. If both throttle devices belong to the same type (orifice or nozzle) then the value ofξ_3/ξ_2 will only depend on the size of these two devices. It will be verified by experiments.

The distributor and measurement system (bypass flow loop) were vertically installed in the left leg of an inverted U-shape pipe, as show in Fig.12. The inner diameter of the pipe was 50 mm, and made from Plexiglas pipe for flow pattern observation purpose. The separator was a cyclone type with an inner diameter of 60 mm. And there was a layer of stainless steel mesh on the top of cyclone cylinder to further remove the small water particle mixed with the gas. The gas flowmeter in the bypass loop was a thermal mass flowmeter (Proline t-mass 65F) with an inner diameter of 15 mm, made by E+H instrument company. and with a measurement accuracy of ±1%. The liquid flow rate was measured with a YOKOGAWA electromagnetic flow meter (ADMAG AE) with an inside diameter of 5 mm and an accuracy of ±0.5% FS.

The two phase flow experimental loop is shown in Fig.13. There were 100 pipe diameters length of straight pipe section upstream of the test section. Air and tap water were used as the working fluids in the experiments. The total air flow rate was metered using a YOKOGAWA vortex flow meter (YF102) with a accuracy of ±1% FS. The total water flow rate was measured with two orifice flow meters with a accuracy of ±1% FS, for lower flow rates and higher flow rates respectively. Since the flow patterns in the inverted U tube were always under an unsteady condition and very difficult to define, we observed the flow regimes at the entrance of inverted U tube i.e. at the horizontal line. The flow pattern occurring during the experiments included stratified flow, stratified wave, slug flow and annular flow. Though the flow pattern observed in horizontal line were not exactly the flow

regime in the inverted U tube before the distributor, it could reflect the effect of flow patterns on the measurement.

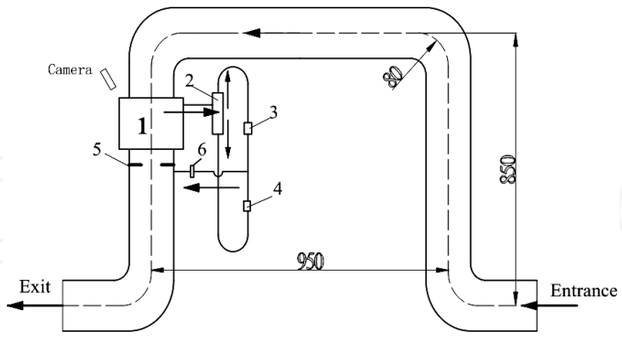

1. Distributor; 2.separator; 3.gas flow meter; 4. liquid flow meter; 5.main throttle; 6.throttle

Fig. 12. Test section

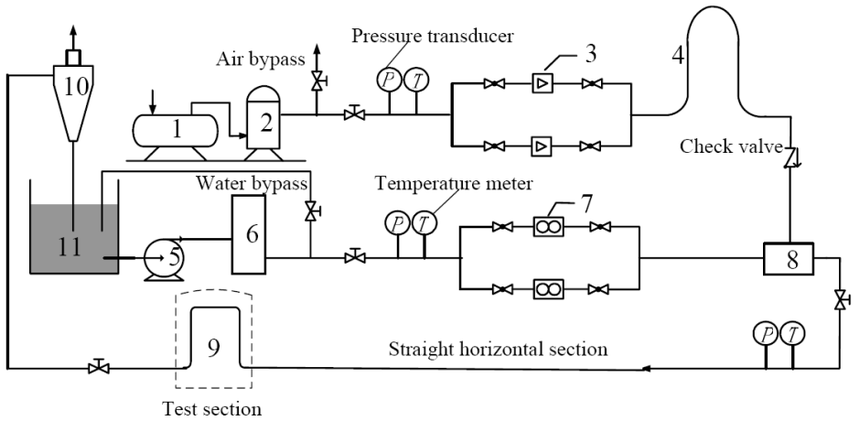

1.Compressor; 2.compressed air vessel; 3.gas flow meter; 4.invertied U tube; 5.Pump; 6. Water vessel; 7.water flow meter; 8.mixer; 9.test section; 10.cyclone separator; 11.water tank

Fig. 13. Two phase flow experimental loop

The electronic signals from instruments and transducers were connected to NI6023E data acquisition system and recorded by a computer. The acquisition frequency was 1kHz and the recording length was 120s. The average values were calculated after the recording. After that the air and water flowrates of total flow and bypass flow were able to be determined, and the real extraction ratio could also be calculated according to Equation (5) and (6). The uncertainty of extraction ratio was less than 1.4% according to the error theory (Taylor, 1982).

For the passive distributor of Fig.10, the wheel was driven by the two-phase flow, and the rotation speed was counted by a high speed video camera recording through the transparent cover of the distributor. Experiments showed that the rotation speed of the wheel was approximately proportional to the velocity of the two-phase mixture. The range of rotation speed of the wheel was 400 to 2000 r/min (T=0.15～0.03 s) with the gas superficial velocity ranged from 8 m/s －22m/s, and the liquid superficial velocity ranged

from 0.02—0.2m/s. The wheel was not able to rotate steadily when the gas superficial velocity was below 7 m/s（at the same time the flow pattern transforms to stratified flow and slug flow.） The flow patterns appeared in this experiment was mainly annular flow. The maximum pressure loss of the distributor was less than 10kpa.

For the active distributor of Fig.11, the wheel was driven by a motor, and the rotation speed was controlled by adjusting the electrical current to the motor. The speed range was 100—700 r/min. The gas superficial velocity range was 1.5 m/s — 8m/s, and the liquid superficial velocity was in the range of 0.02～0.45m/s. The flow patterns occurred in the experiment included stratified flow, slug flow and stratified wave. The maximum pressure loss of the distributor was less than 6kpa.

For the passive distributor of Fig.10, the theoretical value of extraction ratio was 0.05, hence the size of the throttle devices in the bypass loop and main loop should be determined by this value according to Equation (22). Both devices selected were orifice plates. In order to determine their size, we first set the diameter of main loop orifice to 20 mm, then determined the diameter of bypass loop orifice by a tentative method. As the diameter equaled to 4.1 mm, experimental data showed that Equation (22) was met, i.e. the real extraction ratio was nearly equal to 0.05 as shown in Fig.14. Where K_L and K_G are the liquid and gas extraction ratios determined by experiments, U_{SL} is the superficial liquid velocity and U_{SG} is the superficial gas velocity. It can be seen that K_G and K_L are very close to the theoretical value of 0.05 and independent of liquid and gas superficial velocity. The average value of K_G was 0.0506, and the standard deviation was 0.00079; the average value of K_L was 0.0498, and the standard deviation was 0.00166. The maximum difference between K_G and the theoretical value was less than 4%, and the maximum difference between K_L and the theoretical value was less than 6%.

For the active distributor of Fig.11, the theoretical value of extraction ratio was 0.0556, we determined the size of orifices with the same method mentioned above. The diameter of main loop orifice was 25 mm, and the diameter of sample loop orifice was 5 mm. the real extraction ratios are shown in Fig.15. It can be seen that when U_{SL} is lager than about 0.1 m/s, K_G and K_L are very close to the theoretical value of 0.0556 and independent of gas and liquid superficial velocity. The average of K_G was 0.0560, and the average of K_L was 0.0559. But as U_{SL} is less than about 0.1 m/s, both K_G and K_L will deviate below the theoretical value, and the lower the gas and liquid velocity, the smaller the K_G and K_L. This can be explained by the fact that as the superficial velocity of liquid and gas become lower, the dynamic pressure of the jets from the flow path of the wheel (refer to Fig.11C) will become smaller, at a certain point (critical value), the dynamic pressure is not high enough to overcome the resistance of fluid rooms to enable the jets to completely flow into the bypass flow header, and some fluid will preferentially flow back to the main flow loop. Fig.16 shows that this critical value is 400 Pa, and it can also be seen that nearly all points fall on the same line. Based on this critical value we can determine the lowest effective working point of the distributor.

Fig.17 shows the effect of rotation speed on the extraction ratios. It can be seen that K_G is not affected by the rotation speed, but K_L increases with the rotation speed as U_{SL} is less than about 0.1 m/s, due to centrifugal force.

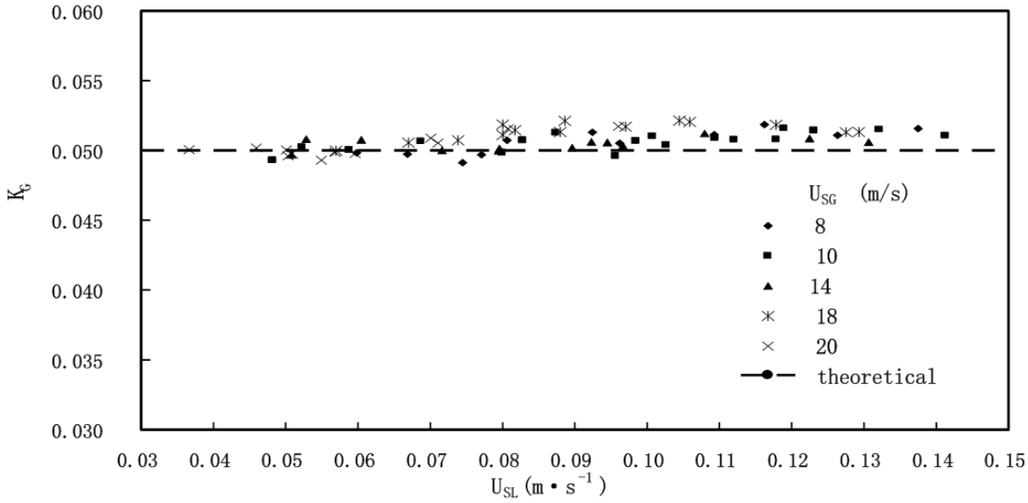

(A)

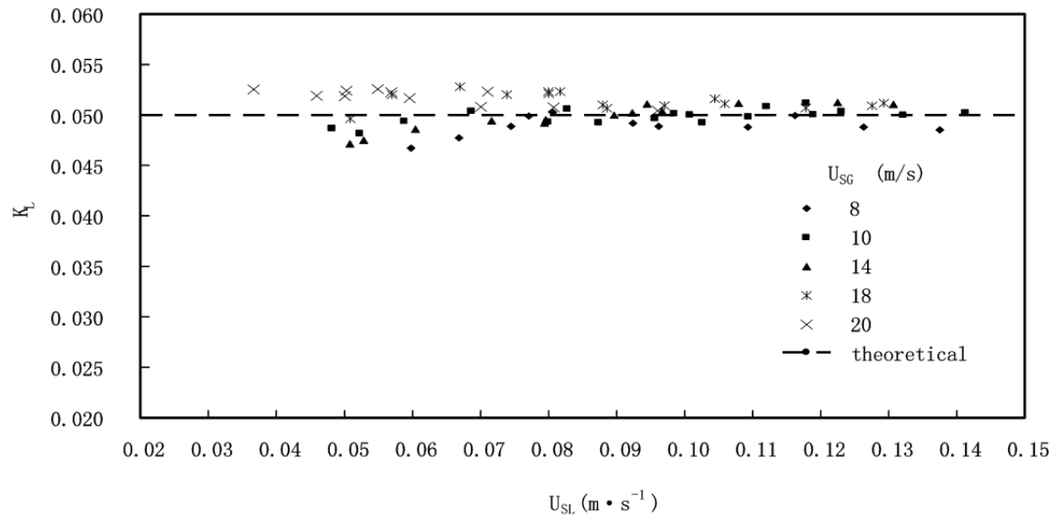

(B)

A: Gas extraction ratio B: Liquid extraction ratio

Fig. 14. Extraction ratios of the passive distributor of Fig.10

Fig.18 shows the effect of flow patterns on the extraction ratios of the active distributor of Fig.11. In the experiments the most frequently occurred flow pattern was slug flow which is the most unsteady flow, from Fig.18 we can see that both K_G and K_L are very close to the theoretical value for all slug flow and some stratified wave data, however, K_G and K_L will drift below the theoretical value as the pattern is stratified flow and for partial stratified wave data. The reason is that in these two patterns both the gas and liquid superficial velocity are lower as compared with other patterns, the jet's dynamic pressure in the wheel is below the critical value of 400 Pa, so some fluids which should flow to bypass loop flow to the main loop. Therefore we can say that it is the jet's dynamic pressure or fluid velocities that affects the K_G and K_L.

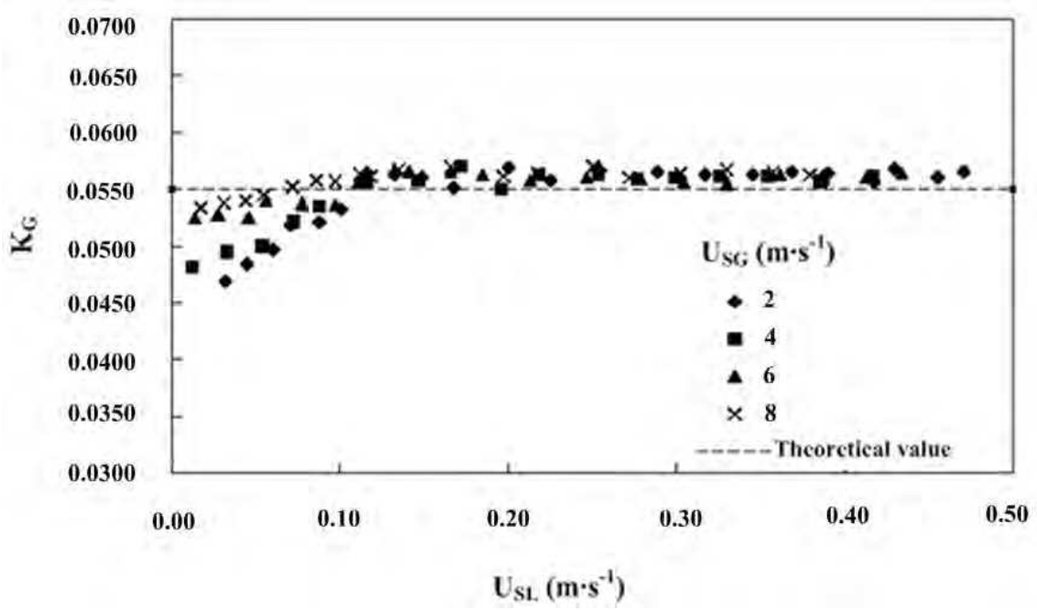

(A)

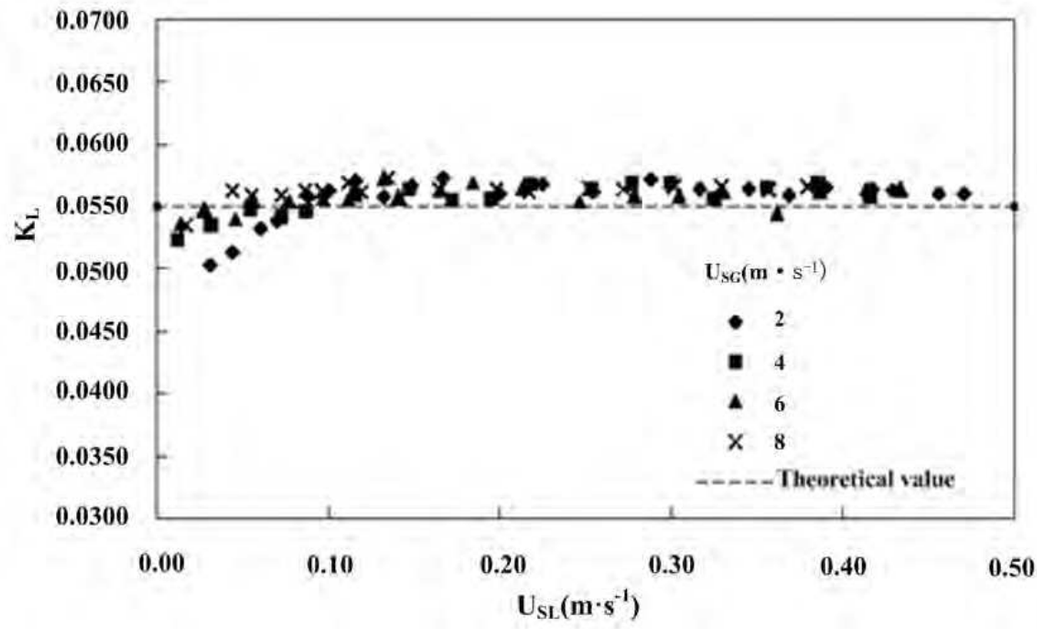

(B)

A: Gas extraction ratio B: Liquid extraction ratio

Fig. 15. Extraction ratios of the active distributor of Fig.11

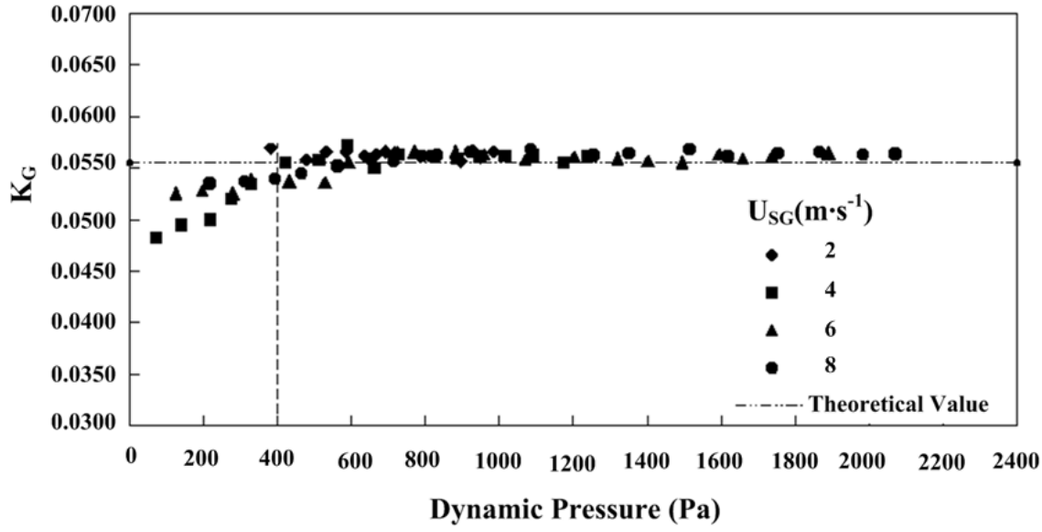

(A)

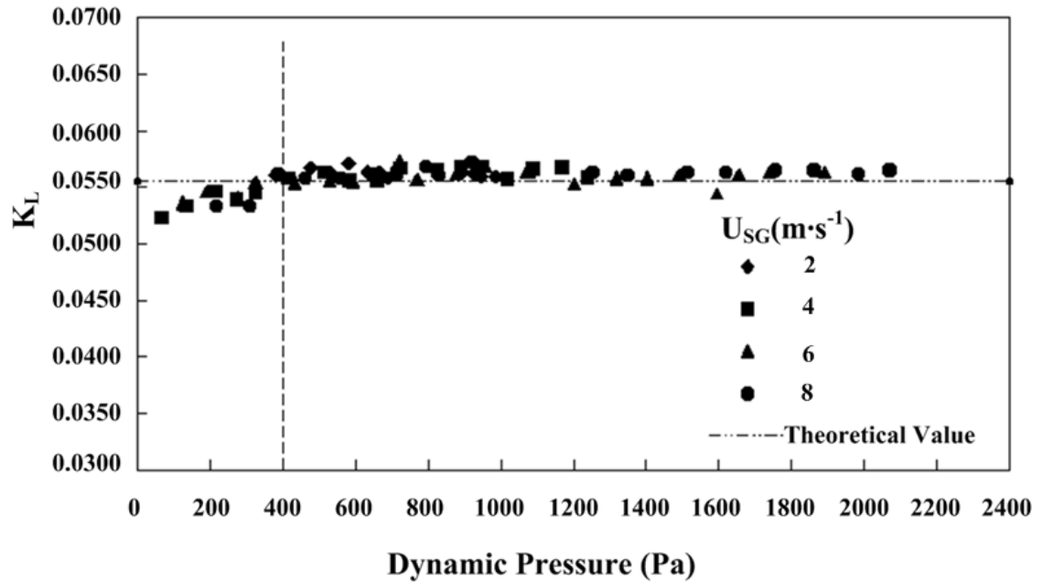

(B)

A: Gas extraction ratio B: Liquid extraction ratio

Fig. 16. Relation between extraction ratios and the jet dynamic pressure

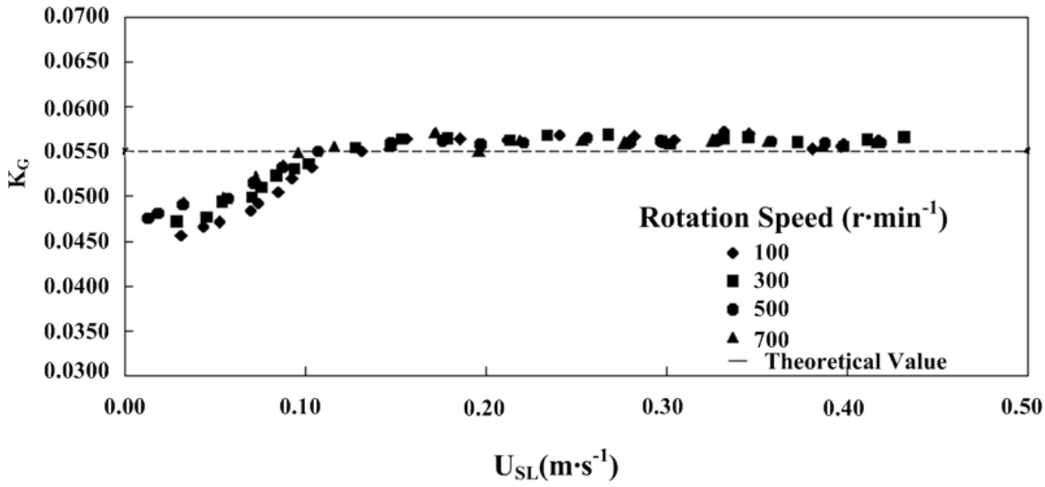

(A)

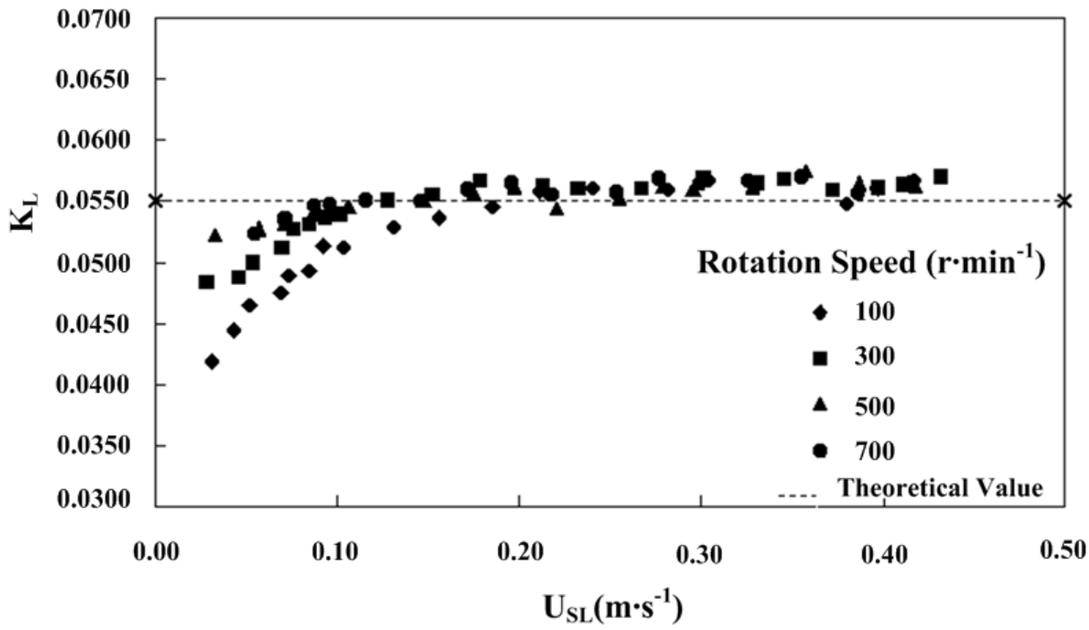

(B)

A: Gas extraction ratio B: Liquid Extraction ratio

Fig. 17. The effect of rotation speed on extraction ratios

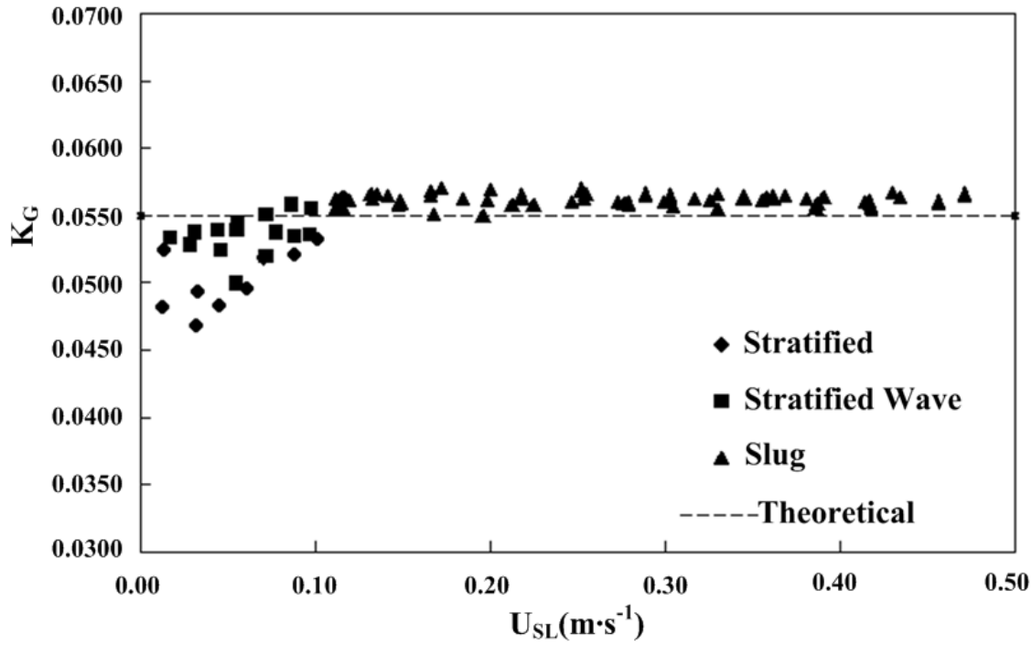

(A)

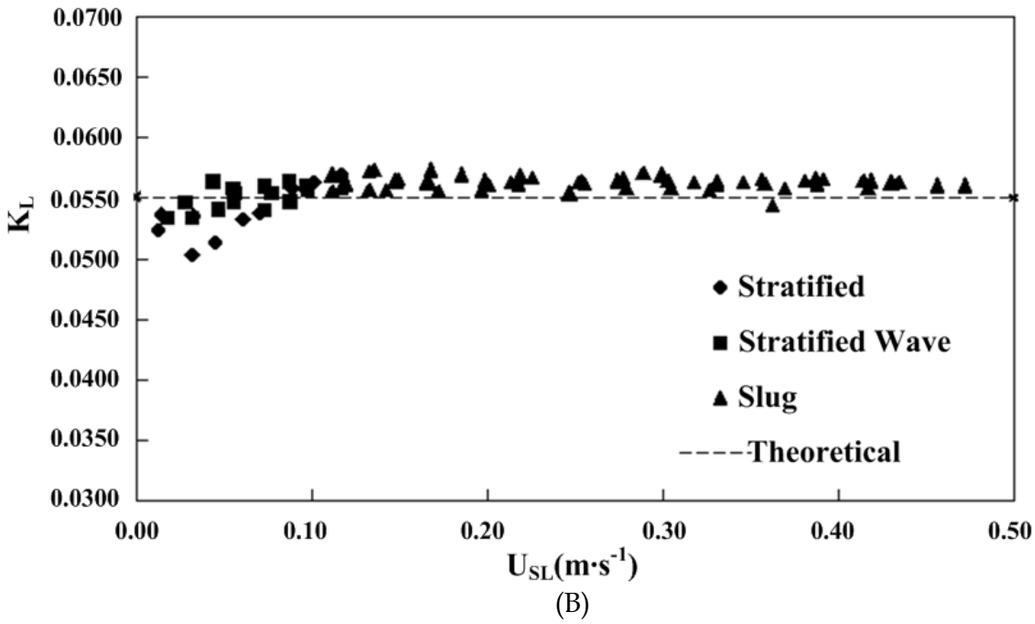

(B)

A: Gas extraction ratio; B: Liquid Extraction ratio

Fig. 18. The effect of flow pattern on extraction ratios

From Fig.14 and Fig.15 we have observed that both K_G and K_L are very close to the theoretical values, i.e. gas and liquid were drawn with the same proportion, so we certainly can expect that the bypass fluid will have the same components as the total flow, and this assumption was proved by the experiments. Comparisons of the gas quality of sample flow

with that of total flow show that the gas quality of sample flow is very close to that of total flow in the experiments, the maximum difference between them is less than 1.3%. This demonstrates that the bypass fluid is an excellent representative of the total flow.

The calibrated values of K_G and K_L which are constants and independent of flowrates can be used to determine the total liquid and gas flow rates M_{1L} and M_{1G} according to Equation (5) and (6) after the bypass flow rate M_{3L} and M_{3G} have been metered. Fig.19 and Fig.20 present the measurement error of total gas and liquid flowrate of two-phase flow respectively. It can be seen that the total flow rates measurements error is less than ±5%，and the large errors occurred at low flowrates. Therefore we can conclude that this method is reliable.

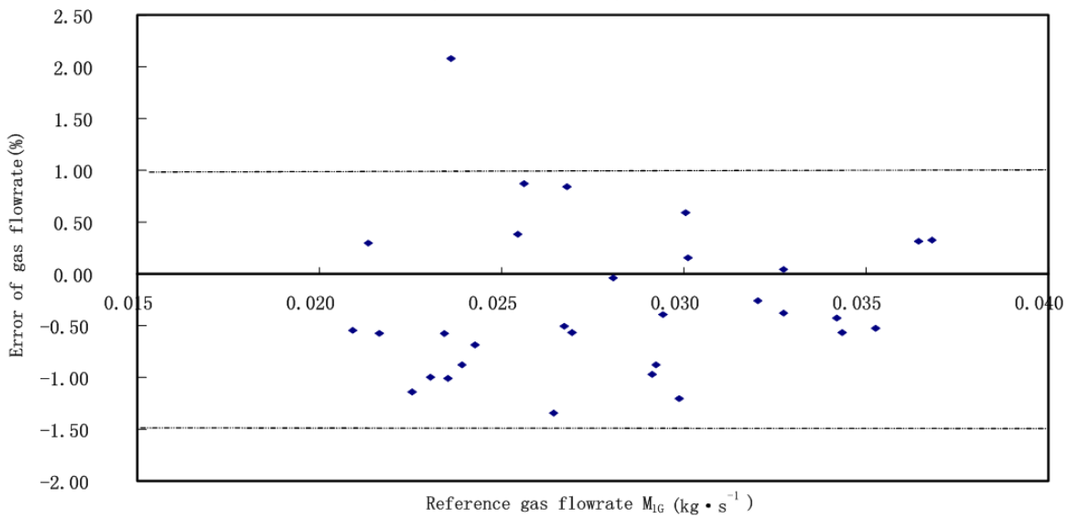

(A)

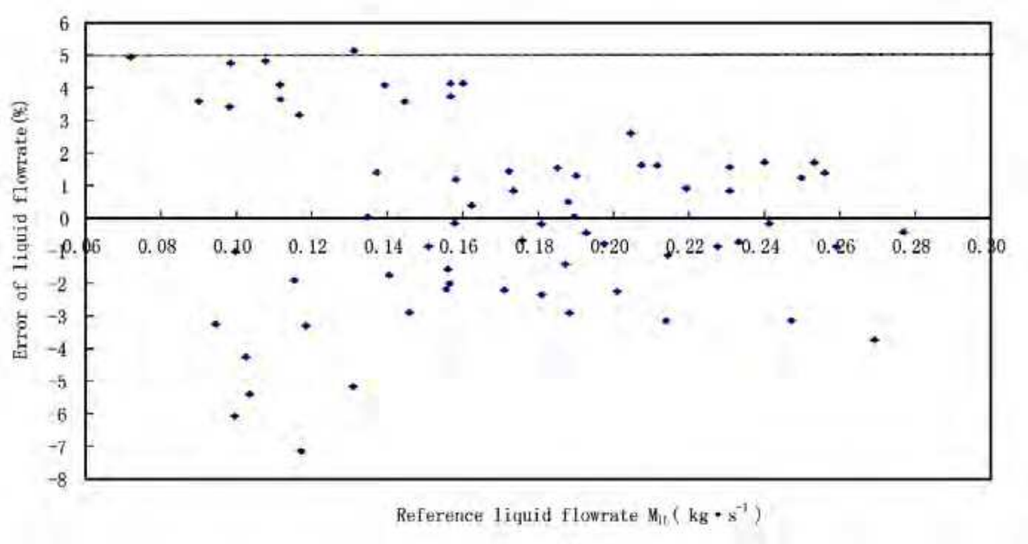

(B)

A: Gas flow B: Liquid flow

Fig. 19. Error of total flowrate measurements of the passive distributor of Fig.10

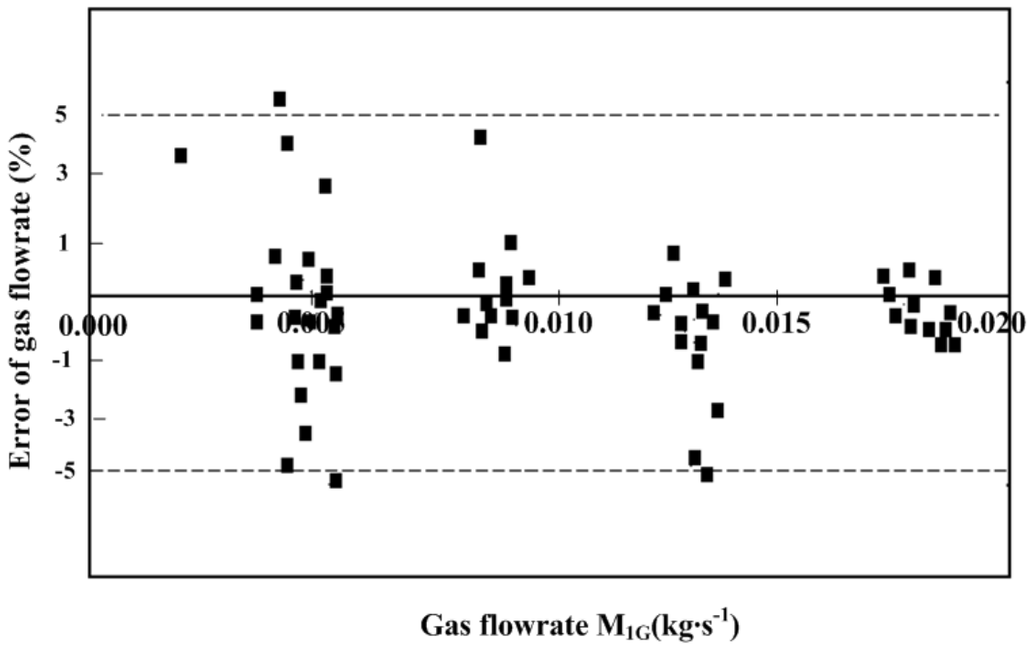

(A)

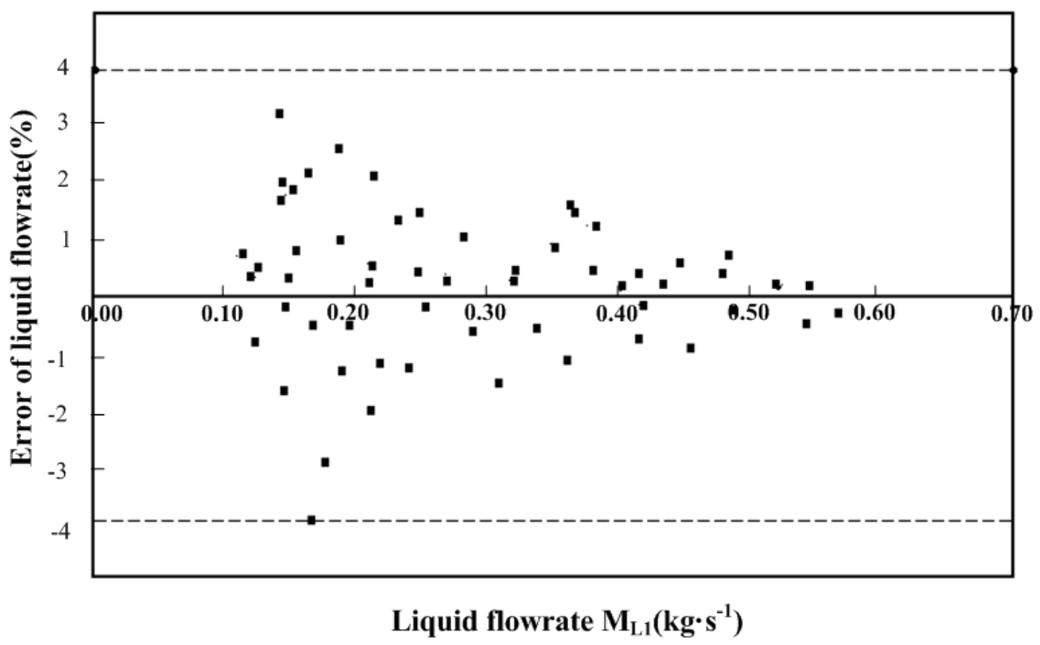

(B)

A: Gas flow B: Liquid flow

Fig. 20. Error of total flowrate measurements of the active distributor of Fig.11

2.3.3 Static distributor for high pressure steam-water two-phase flow

In high pressure steam-water flow condition, it is more suitable to use a static distributor that does not contain any moving parts. A distributor used in this study is shown in A-A section view of Fig.21 (Wang et al, 2011).

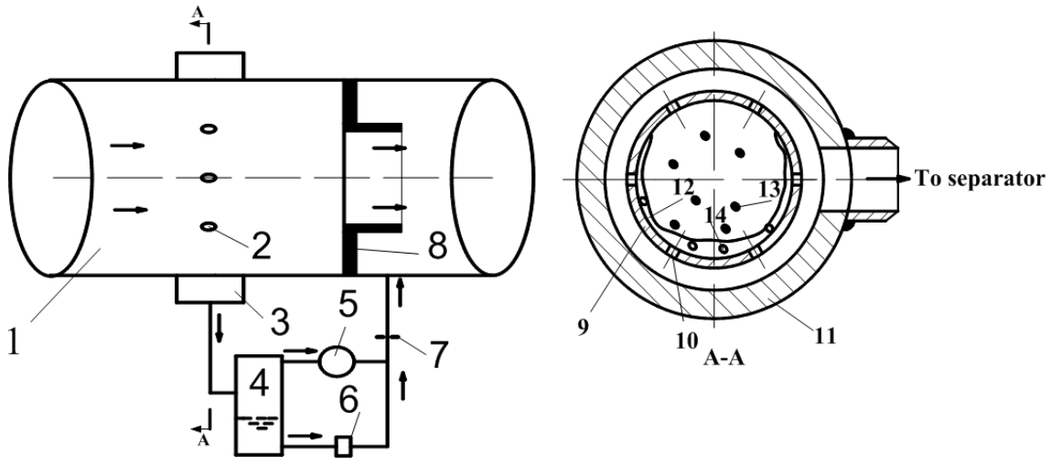

1. main pipe; 2,10.division holes; 3.collection ring; 4.separator; 5.steam meter; 6.water meter; 7.throttle device; 8.main loop throttle device; 9.pipe wall;11.the wall of collection ring;12.water film;13.water droplet;14.steam bubble

Fig. 21. Static distributor and flow division system

The static distributor consists of 6 small division holes that are evenly spaced around the circumference of the main pipe and a collection ring surrounding the pipe wall. The inside diameter of the main pipe was 50 mm, and the thickness of the pipe wall was 3 mm. The inner diameter of the collection ring was 70 mm, and the diameter of the division hole was 3.5 mm. The separator is a cyclone type with inner diameter of 42 mm. Both the steam meter and water meter were venturi tubes with throat diameter of 7.4 mm and 4.4 mm respectively. The throttle device was a thick orifice plate with diameter of 3.5 mm. The restriction in main loop was a nozzle with diameter of 28 mm.

To be equivalent to equation (5) and (6), the total steam and water flow rates are determined by the following equations

$$M_s = \frac{M_{ss}}{K_s} \tag{23}$$

$$M_w = \frac{M_{sw}}{K_w} \tag{24}$$

Where, M_s is the total steam flow rate; M_w is the total water flow rate; M_{ss} is the bypass steam flow rate metered by steam meter; M_{sw} is the bypass water flow rate metered by water meter; K_s is the steam extraction ratio; K_w is the water extraction ratio. Referring to Fig.21, we can also see that the fluid flowing to the division (bypass) loop comes from a region near the wall where the water proportion is higher, and therefore more water will enter the division loop, i.e. K_w will be larger than K_s, and it is beneficial to the measurement of water flow rate in the condition of flow with high steam volume fraction.

Equation (23) and (24) are only the definition of extraction ratios, the real values of K_s and K_w are dependent on the resistance relation between the division (bypass) loop and the main loop, and also on the distribution characteristic of the division loop. From Fig.21 we can see that the division (bypass) loop and the main loop have a common inlet and a common outlet, i.e. they are in parallel. In accordance with the nature of parallel loops (Munson, 2002), the pressure losses of both loops are equal

$$\Delta P_m = \Delta P_s \tag{25}$$

Where, ΔP_m is the pressure loss in the main loop; ΔP_s is the pressure loss in the division (bypass) loop.

ΔP_m and ΔP_s can be calculated based on the separated flow model (Lin, 1982)

$$\sqrt{\Delta P_m} = \sqrt{\Delta P_{ms}} + \theta_m \sqrt{\Delta P_{mw}} \tag{26}$$

$$\sqrt{\Delta P_s} = \sqrt{\Delta P_{ss}} + \theta_s \sqrt{\Delta P_{sw}} \tag{27}$$

Where, ΔP_{ms} and ΔP_{mw} are the pressure losses when steam phase and water phase flows in the main loop alone respectively; ΔP_{ss} and ΔP_{sw} are the pressure losses when steam phase and water phase flows in the division loop alone respectively; θ is the correction factor which depends on the pressure (Lin, 1982).

In accordance with the single phase flow pressure loss calculation method (Munson, 2002), we can write down the following equations

$$\Delta P_{ms} = \left[\sum \lambda_m \frac{1}{d_m} + \sum \xi_m \right] \frac{1}{2\rho_s} \left(\frac{M_{ms}}{A_m} \right)^2 \tag{28}$$

$$\Delta P_{mw} = \left[\sum \lambda_m \frac{1}{d_m} + \sum \xi_m \right] \frac{1}{2\rho_w} \left(\frac{M_{mw}}{A_m} \right)^2 \tag{29}$$

$$\Delta P_{ss} = \left[\sum \lambda_s \frac{1}{d_s} + \sum \xi_s \right] \frac{1}{2\rho_s} \left(\frac{M_{ss}}{A_s} \right)^2 \tag{30}$$

$$\Delta P_{sw} = \left[\sum \lambda_s \frac{1}{d_s} + \sum \xi_s \right] \frac{1}{2\rho_w} \left(\frac{M_{sw}}{A_s} \right)^2 \tag{31}$$

Where, λ is the Darcy friction factor, l is the tube length, d is the tube inner diameter, ξ is the local loss factor, ρ_w is the density of water, ρ_s is the density of steam, M is the mass flowrate, A is the tube cross section area, the symbol Σ represents summation; subscript "m" represents the main loop and the subscript "s" represents the division loop.

Based on mass conservation, we can write down the flow rates relation of the total flow with that in the main loop and the division (bypass) loop

$$M_s = M_{ms} + M_{ss} \tag{32}$$

$$M_w = M_{mw} + M_{sw} \tag{33}$$

Let X_m be the steam quality of the main loop, X_s be the steam quality of division loop, and neglect the little difference between θ_m and θ_s i.e. $\theta_m=\theta_s=\theta$, then substituting equations (23)-(24) and (26)-(33) into (25), one can obtain

$$\frac{K_0}{K_s}-1=\theta\left(1-\frac{K_0}{K_w}\right)\sqrt{\frac{\rho_s}{\rho_w}}\left(\frac{1}{X_s}-1\right) \tag{34}$$

Where K_0 is the extraction ratio in the case of single phase flow, which can be calculated by the following equation or determined by experiments

$$K_0=\frac{A_s\sqrt{\sum\lambda_m\frac{1}{d_m}+\sum\xi_m}}{A_s\sqrt{\sum\lambda_m\frac{1}{d_m}+\sum\xi_m}+A_m\sqrt{\sum\lambda_s\frac{1}{d_s}+\sum\xi_s}} \tag{35}$$

Equation (34) is known as the resistance equilibrium equation because it is derived from the resistance relation, however, it alone cannot yet determine the values of K_s and K_w, therefore another additional equation must be developed, and equation (34) is the first equation for extraction ratios. Define K_m as the mass extraction ratio

$$K_m=\frac{M_{ss}+M_{sw}}{M_s+M_w}=\frac{1}{\frac{X_s}{K_s}+\frac{1-X_s}{K_w}} \tag{36}$$

For a given structure of the main loop and the division loop, K_m is usually a constant in the case of single phase flow, however in the condition of two phase flow, K_m may vary with the flow rate and steam quality, therefore the value of K_m/K_0 is the function of flow rate and steam quality

$$\frac{K_m}{K_0}=F(M,X_S) \tag{37}$$

The function $F(M,X_S)$ reflects the distribution characteristic of division loop, and can only be determined by experiments.

Experiments were carried out in an once-through boiler for steam flooding in Keramay oilfield, Xinjiang China. Fig.22 is the schematic representation of the experimental systems. The experimental setup was horizontally installed at the test section. The length of the straight horizontal pipe between the sampler separator and test section was 3 meters, and the length of division steam pipe was 0.68 meters. All the pipe and test section were properly insulated with mineral fiber. The heat loss rate in the main pipe and division loop, based on a heat transfer calculation, were less than 0.15kw/m and 76w respectively, and the steam condensation due to heat loss were less than 0.41kg/(m・h) and 0.13kg/h respectively, both were insignificant compared to the steam flow in the pipe.

The flow rate to the once-through boiler was adjusted by changing the rotation speed of the piston pump with a frequency converter, and metered by a calibrated orifice flow meter at the entrance of the boiler which has an accuracy of 1.3%. In accordance with the nature of once-through boiler, the flowrate throughout the boiler must keep a constant in the condition of steady state, because in the steady state the amounts of fluids (water and steam)

within the boiler have reached their stable values, no additional fluid will accumulate or be removed from the boiler, i.e. the input must equal to the output. So the flowrate passing through the test section can be measured by the orifice flow meter at the entrance of the boiler under steady state.

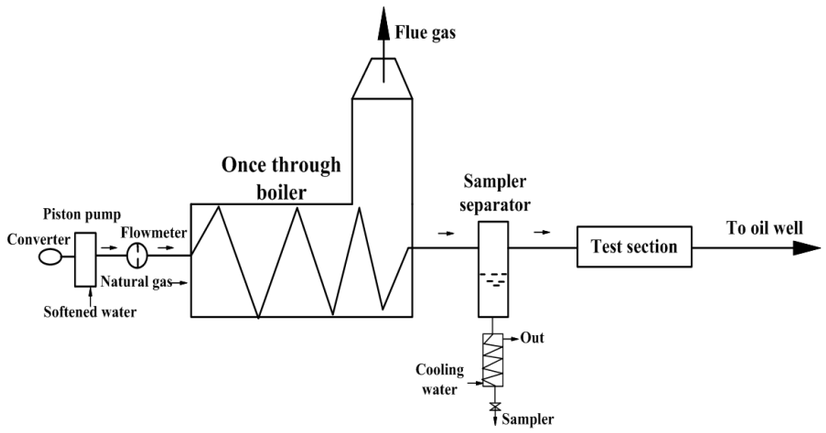

Fig. 22. Schematic representation of the experimental setup

The output steam quality of the boiler was carefully controlled by adjusting the flow rate of natural gas entering the furnace. The value of steam quality at the boiler output was determined based on the fact that the salts dissolved in the softened water (Na_2SO_4, Na_2SiO_3, et al.) still remain in water after the evaporation process in boiler, hence, according the salts conservation, we can write down the following equations

$$M \cdot S_i = M \cdot (1 - X) \cdot S_o \tag{38}$$

$$X = \frac{S_o - S_i}{S_o} \tag{39}$$

Where，S_i is the salts concentration of softened water at the input of the boiler; S_o is the salts concentration of condensed water at the output of the boiler, i.e. at the sampler separator. The sampler separator of Fig.22 is a small vessel connected to the steam pipe which is used to collect some water from the steam-water flow by gravitational effect, but not designed to separate the whole steam-water flow. A very small amount of water(less than 8kg/h) is drained from the sampler separator and then cooled by cooling water, this is the sampler of condensed water.It should be noted that equation (38) and equation (39) are correct only in the condition of steady state of the boiler operation. Due to this reason we had to wait for 2-3 hours after an adjustment of boiler parameters (flowrate or quality) to ensure that a steady state had been reached before the measurements of flowrate and steam quality were able to be taken.

Equation (39) is not convenient to use because it is not an easy task to measure the salts concentration directly in oilfield. The salts concentration measurements are usually replaced by that of electrical conductivity in oilfield based on the principle that in the case of low salts concentration (far below their solubility), the molar conductivity (the conductivity per unit of concentration) tends to be a constant(Aguado, 2006), hence the conductivity of water is proportional to the salts concentration, so Equation (39) can become as

$$X = \frac{C_o - C_i}{C_o} \tag{40}$$

Where, C_i is the softened water conductivity at the input of the boiler; C_o is the condensed water conductivity at the output of the boiler, i.e. at the sampler separator.

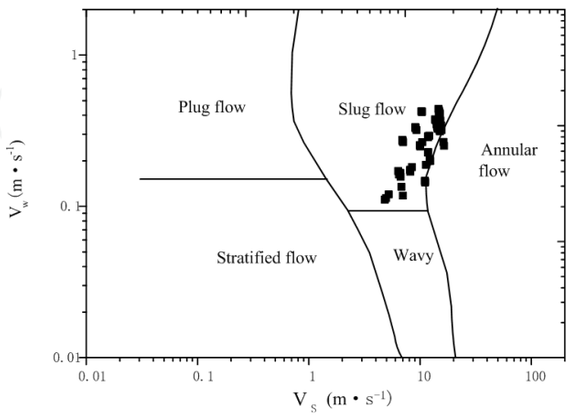

Fig. 23. Experimental range

Equation (40) has been successfully used to measure steam quality in oilfield for many years. During the experiments,both C_i and C_o were measured by a portable conductivity meter with an accuracy of 0.5%, according to error theory, the error of steam quality from Equation (40) is 0.6%. For the sake of boiler safety, the lowest steam quality allowed was 0.60, and the highest steam quality allowed was 0.82 and this range of steam quality is enough to cover the quality usually encountered in oilfield. The flow rate range was 2000kg/h to 8000kg/h, and pressure range was 7.6MPa to 16MPa. Fig.23 showed the experiments range in the Mandhane map (Collier,1981), where V_s represents the superficial steam velocity, and V_w the superficial water velocity. From Fig.22 we can see that the experiment points were mainly located on the borders of slug flow, annular flow and wavy flow which are the most frequently occurring regimes in the steam pipe line for the steam flooding and other industries.

The static pressure of the test section was measured by a Rosemount 3051 pressure transmitter, and both the steam venturi tube and water venture tube differential pressures in the division loop was measured by a Rosemount 3051 differential pressure transmitter respectively. These three transmitters' signals were connected to an industrial computer which automatically converts the signals to numerical data and calculate the bypass steam and water flow rates.

Before the normal two phase flow experiments, a single phase water flow experiment was conducted to determine the value of K_0 (the extraction ratio in single phase case), the result was K_0=0.01350. During the two phase experiments, the pressure and bypass steam and water flow rates were automatically recorded by the computer, and the extraction ratios was able to be calculated according to equation (23) and (24) once the flow rate of the boiler and the steam quality were measured. The results of extraction ratios is shown in Fig. 24, where the horizontal axis represents the right term of equation (34), and the vertical axis represents the left term of equation (34). From Fig.24 it can be seen that a liner relationship exists between the ordinate and the abscissa, and all the experimental points fall on the same line, it means that the equation (34) is correct and independent of flow rate. From these data we can also obtain the value of θ=1.6259.

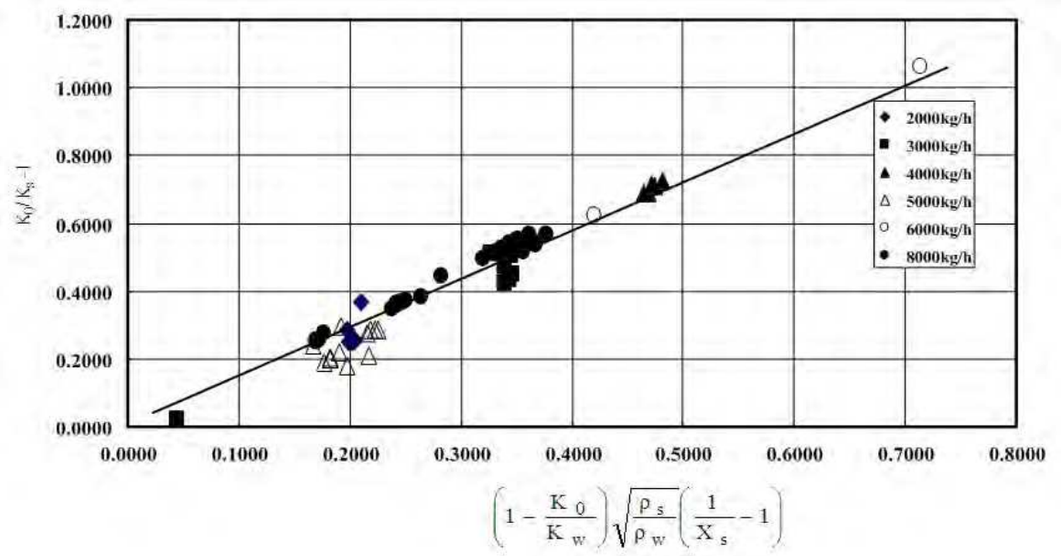

Fig. 24. Experimental results of extraction ratios

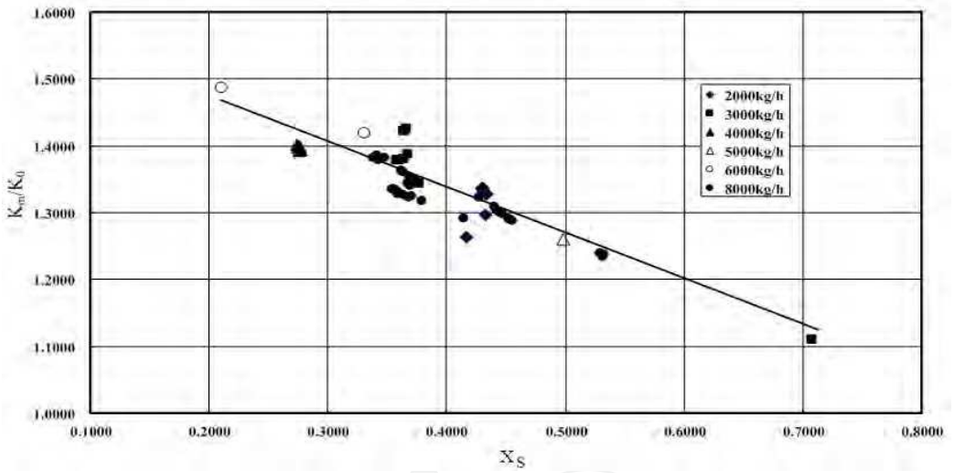

Fig. 25. Relationship between K_m and X_s

Fig.25 showed the relationship between the mass extraction ratio K_m and steam quality of bypass loop X_s for various mass flow rates. It can be seen that a simple linear relation exists between them, and all the experimental data fall on the same line, this means that flow rate M has little effect on the $F(M,X_s)$. From these data the actual form of $F(M,X_s)$ in equation (37) can be determined

$$\frac{K_m}{K_0} = F(M, X_S) = 1.6090 - 0.6919X_s \tag{41}$$

Substituting equation (41) into equation (36) one can obtain

$$\frac{K_0}{K_s}X_s + \frac{K_0}{K_w}(1 - X_s) = \frac{1}{1.6090 - 0.6919X_s} \tag{42}$$

Equation (42) is the second equation of extraction ratios and is called the distribution equation because it reflects the distribution nature of bypass loop.

The extraction ratios K_s and K_w can now be determined by solving equation (34) and (42), and then the total steam and water flow rate M_s and M_w(or the total flow rate M and quality X) can be measured once the bypass steam and water flow rate M_{ss} and M_{sw} are metered, these works are automatically done by the computer which is connected to the pressure and different pressure transmitters. Table 1 give some measurement results, where the reference flowrates represent values metered by the orifice flowmeter at the entrance of the boiler, the reference mass quality is obtained by conductivity method. From Table 1 it can be seen that the maximum error of flow rate measurements is less than ±2.5%, and the maximum error of quality measurements is less than ±3.5%. The water extraction ratio K_w is 3~5 times more than steam extraction ratio K_s.

No	Flow rate (kg/h)			Mass quality			Extraction ratio	
	Measured	Reference	Error(%)	Measured	Reference	Error(%)	K_s	K_w
1	2120	2100	0.95	0.7236	0.7200	0.36	0.01075	0.03677
2	3430	3420	0.29	0.7975	0.8000	-0.25	0.01325	0.02195
3	3930	4000	-1.75	0.6980	0.6628	3.52	0.007828	0.04072
4	4890	4850	0.82	0.6403	0.6517	-1.14	0.006811	0.04552
5	5160	5150	0.20	0.7788	0.8140	3.52	0.01096	0.04587
6	6130	6150	-0.33	0.6636	0.6473	1.63	0.006541	0.04489
7	7438	7529	-1.21	0.7651	0.7758	-1.07	0.008774	0.05089
8	7540	7600	-0.79	0.7746	0.7541	2.05	0.008852	0.04667
9	7880	8070	-2.35	0.7564	0.7403	1.61	0.008750	0.04242
10	7990	8070	-1.00	0.7837	0.7886	-0.49	0.09423	0.04783

Table 1. Measurement results of flow rate and mass quality

3. Conclusion

Flow division techniques have been widely used in single phase flow measurements, whose main feature is to utilize a small size meter to measure a large volume flow in large lines. In addition to this, a bypass flow meter usually has a much wider metering range, a better precision and a lower price. Further more, when we apply this technique in two-phase flow, an even more important advantage will appear: a small size separator can be used in the bypass loop to separate the two-phase mixture and consequently measuring them by conventional single phase meters, thus the problem of two-phase flow rate measurement can simply be solved. However a special distributor must be employed to ensure that the bypass flow will have the same components as the total flow and be proportional to the total flow. Three different kinds of distributors have been studied in this chapter.

The rotational drum is a flow driven distributor whose extraction ratio is equal to the ratio of extraction channel number to the total flow channel number and independent of flow patterns. The gap size between the drum and the shell has a significant effect on the real extraction ratios. When the gap size is equal to 0.25 mm, a much stable extraction ratio can be obtained. The measurements error of total flow is less than $\pm$5.6%. Experiments also showed that the drum rotation speed has no effect on the measurement.

The wheel-fluid rooms distributor is much simpler in structure. The wheel can be driven either by the flow or by a motor and the rotation speed has no effect on the measurements. The extraction ratio can be as low as 0.05 (and 0.0556) and depends only on the ratio of bypass fluid room number to the total fluid room number. The superficial gas velocity can be as low as 1.5 m/s, and the measurement error of total flow rate is within ±5% in the above experimental ranges.

The static distributor was specially designed for the high pressure steam-water two-phase flow measurements where any moving parts in the apparatus may reduce the reliability of the meter. Although the static distributor can not keep the extraction ratio as a constant as the rotational drum or the wheel- fluid rooms distributor does, two independent equations about the extraction ratios have been derived from the resistance equilibrium relation between the main loop and bypass loop, and the distribution function respectively. Thus the extraction ratios can be determined by solving these two equations. The extraction ratios were as small as 0.007-0.05 which is very important to the development of high pressure two-phase flow meter. The experiment points were mainly located on the borders of slug flow, annular flow and wavy flow in the Mandhane map. The error of flow rate measurements is less than ±2.5%, and the error of quality measurements is less than ±3.5%.

4. Acknowledgment

The authors express their great thanks to National Natural Science Foundation of China for financial support (No.50776071 and No.50376051), and also to Dr. Y B Yang and Ms R P Wang for their careful language revision.

5. References

Adams, M. M. (1969). Electric thermal flowmeter. Us Patent :3425277

Aguado, D. ; Montoya, T. ; Ferrer, J. & Seco, A. (2006).Relating ions concentration variations to conductivity variations in a sequencing batch reactor operated for enhanced biological phosphorus removal. *Environmental Modelling & Software,* Vol.21,No.6, (March 2005), pp.845-851，ISSN: 1364-8152

Bahrton, G. (1996). Flowmeter with a variable constriction. Us Patent :5554805

Baker, W. C. (1969). Fluid flow measuring appratus. Us Patent :3443434

Baker, W. C .(1971). Fluid flow measuring appratus. Us Patent :3559482

Baker, W. C. (1977). Fluid flowmeter. Us Patent :4041757

Bates, C. J. & Ayob, R. (1995). Annular two-phase flow measurements using phase Doppler anemometry with scattering angles of 30° and 70°. *Flow Meas. Instrum*. Vol.6,No.1,(January 1994), pp.21-28,ISSN: 0955-5986

Beg, N. A.&Toral, H. (1993). Off-site calibration of a two-phase pattern recognition flowmeter. *Int. J. of Multiphase Flow*,Vol.19, No.6,pp.999-1012, ISSN: 0301-9322

Butterworth, D. & Hewitt, G. F. (1978). *Two-phase flow and heat transfer*, Oxford University Press,pp.49, ISBN:0-19-851715-7, Oxford, UK.

Cha, J. E. ; Ahn, Y. C. & Kim, M. H. (2002). Flow measurement with an electromagnetic flowmeter in two-phase bubbly and slug flow regimes. *Flow Meas. Instrum.* Vol.12,No.5, (January 2002), pp.329–339, ISSN: 0955-5986

Chisholm, D. (1974). Pressure drop during steam/water flows through orifices *J. Mech. Eng. Sci.* Vol.16, No.5, pp.353-355, ISSN: 0022-2542

Collier, J. G.(1981).*Convective Boiling and Condensation* (second edition),McGRAW-HILL International Book Company, pp. 6-21, ISBN :0-07-011798-5, Berkshire,England

Connet, F. N. (1928). Proportionate meter. Us Patent :1681762

DeCarlo, J. P. (1984). *Fundamentals of flow measurement*, Instrument Society of America, pp.195-199, ISBN : 0-87664-627-5, North Carolina, USA

Fenelon, P. J.(1994). In-line parallel proportionally partitioned by-pass metering device and metering device and method. Us patent :533496

Ferreira, V. C. S. (1997).Differential pressure spectral analysis for two-phase flow through an orifice plate. *Int. J. Pres. Ves. & Piping,* Vol.73, No.1, pp.19-23, ISSN: 0308-0161

Geng, Y. F.;Zheng. J. W. & Shi, G. (2007). Wet Gas Meter Development Based on Slotted Orifice Couple and Neural Network Techniques. *Chin. J. Chem. Eng.* Vol.15,No. 2,pp. 281-285, ISSN: 1004-9541

Hawk, C. E. (1984). High temperature mass flowmeter. Us Patent :4475387

Hirst, C. D. (1956). Proportional water meter.Us Patent :2750797

Hodgson, J. L. (1932).Flow quantity meter.Us Patent :1870849

Huang, Z. Y.; Xie, D. L., Zhang, H. J. & Li, H. Q. (2005). Gas–oil two-phase flow measurement using an electrical capacitance tomography system and a Venturi meter. *Flow Meas. Instrum.* Vol.16,No.2 ,pp.177-182, ISSN: 0955-5986

Jung, S. H.; Kim, J. S.; Kim, J. B. & Kwon, T. Y. (2009). Flow-rate measurements of a dual-phase pipe flow by cross-correlation technique of transmitted radiation signals. *Applied Radiation and Isotopes* ,Vol.67,No.7, pp.1254-1258 , ISSN: 0969-8043

Kalotay, P. Z. (1994). In-flow Coriolis effect mass flowmeter. Us Patent :5347874

Kane, M. (1994). Hydrodynamic fluid divider for fluid measuring device. Us Patent :5297426

Kidder, H. H. (1934). Water meter for pipe line systems. Us Patent :1954386

Kriiger, G. J.; Birke, A. & Weiss, R. (1996). Nuclear magnetic resonance (NMR) two phase mass flow measurements. *Flow Meas. Instrum.*,Vol.7,No.1,pp. 25-37, ISSN: 0955-5986

Kronberger, H. (1952). Arrangement for measuring or indicating the flow of fluids. Us Patent :2586060

Laub, J. H. (1956). Thermal flowmeter. Us Patent :2729976

Lin, Z. H. (1982). Two-phase flow measurements with sharp-edged orifices. *Int. J. Multiphase Flow,* Vol.8, No.6, pp. 683-693, ISSN: 0301-9322

Lin Z. H., Wang S. Z. and Wang D.(2003). *Gas-liquid two-phase flow and boiling heat transfer,* Xi'an Jiaotong university Press, pp.63-187, ISBN:7-5605-1656-4,Xi'an,China.

Liou, K. T. (1995). Multiphase flow separation and measurement system. Us patent:5390547

Meng, Z. Z.; Huang, Z. Y.; Wang, B. L.; Ji, H. F.;Li, H. Q. & Yan, Y. (2010). Air_water two-phase flow measurement using a Venturi meter and an electrical resistance tomography sensor. *Flow Meas. Instrum.* Vol.21, No.3, pp.268-76, ISSN: 0955-5986

Meribout, M.; Nabeel, A. R. ;Ahmed, A. N.; Ali, A. B. ; Khamis, A. B. & Adel, M. (2010).Integration of impedance measurements with acoustic measurements for accurate two phase flow metering in case of high water-cut. *Flow Meas. Instrum,* Vol.21,No.1 ,pp.8-19, ISSN: 0955-5986

Munson, B. R.; Yang, D. F. & Okiishi,T. H.(2002). *Fundamentals of fluid Mechanics* (Fourth Edition), John Wiley & Sons Inc., pp.475-510, ISBN:0-471-44250-X, New york,USA

Murdock, J. W. (1962). Two-phase flow measurements with orifices . *J. Basic Eng*. Vol.84, No.4, pp. 419-33, ISSN: 0021-9223

Olin, J. G. (1984). Multirange flowmeter. Us Patent :4461173.

Oliveira, J. L. G.; Passos, J. C.; Verschaeren, R. & Geld, C. V. D. (2009). Mass flow rate measurements in gas-liquid flows by means of a venturi or orifice plate coupled to

a void fraction sensor. *Experimental Thermal and Fluid Science*,Vol.33, No.2 pp. 253-60, ISSN: 0894-1777

Peranio, A, (1967). Shunt flow meter. Us Patent :3314290

Reis, E. D. & Jr, L. G. (2008). On the measurement of the mass flow rate of horizontal two-phase flows in the proximity of the transition lines which separates two different flow patterns. *Flow Meas. Instrum.*,Vol.19, No.5,pp.269-82, ISSN: 0955-5986

Rlkuta, S. (1969). Flow meter of the area type. Us Patent :3603148

Sato, K. (1983). Gas flow measuring appratus. Us Patent :4381668

Skea, A. F. & Hall, A. W. R. (1999). Effects of water in oil and oil in water on single-phase flowmeters. *Flow Meas. Instrum.* Vol.10, No.3, pp. 151-157, ISSN: 0955-5986

Stenberg, N. K. (1962). Rate of flow indicator. Us Patent :3066530

Steven, R. & Hall, A. (2009). Orifice plate meter wet gas flow performance. *Flow Meas. Instrum.*Vol.20, No.4, pp.141-51, ISSN: 0955-5986

Steven, R. N. (2002). Wet gas metering with a horizontally mounted Venturi meter. *Flow Meas. Instrum.* Vol.12, No.5, pp. 361-72, ISSN: 0955-5986

Sun, Z. Q. (2010). Mass flow measurement of gas–liquid bubble flow with the combined use of a Venturi tube and a vortex flowmeter. *Meas. Sci. Technol.* Vol.21, No.5, pp. 055403:1-7, ISSN:0957-0233

Taylor, J. R. (1982). *An introduction to error analysis The study of uncertainties in physical measurements*, University Science Books,pp.57, ISBN: 0-935702-10-5, California, USA

Thomson, J. (1895a). Proportional water meter.Us Patent :535639

Thomson, J. (1895b). Proportional water meter.Us Patent :535642

Thorn, R.; Johansen, G. A. &Hammer, E. A. (1997). Recent development in three-phase flow measurement. *Meas. Sci. Technol.,* Vol.8, No.7, pp.691-701, ISSN:0957-0233

Turkowski, M. (2004). Simple installation for measurement of two-phase gas-liquid flow by means of conventional single-phase flowmeters. *Flow Meas. Instrum.*,Vol.15, No.5,pp.295-99, ISSN: 0955-5986

Van, C. C. B. (1999). Bypass type Coriolis effect flowmeter. Us Patent :5861561

Wang, D. & Lin, Z. H. (2002). Gas-liquid Two-phase Flow Measurement Using ESM. *Experimental Thermal and Fluid Science* ,Vol.26,No.6 ,pp.827-32, ISSN: 0894-1777

Wang, D.; Liang, F. C.; Zhang, X. G. & Lin, Z. H. (2012). Multiphase flow measurements by full batch sampling. *Int. J. of Multiphase Flow*, Vol.40, No.4, pp.113-125, ISSN: 0301-9322

Wang, D.; Tan, J. P. & Lin, Y. (2011). High pressure steam water two-phase flow measurement by flow division and separation method. *Proceedings of the 7th international symposium on measurement techniques for multiphase flows,* Tianjin China, 9, 2011

Wang, W. R. & Tong, Y. X. (1995). A new method of two-phase flow measurement by orifice plate differential pressure noise. *Flow Meas. Instrum.* Vol.6,No.4, pp.265-270, ISSN: 0955-5986

Xu, L. J. ; Xu, J.; Dong, F. & Zhang, T. (2003). On fluctuation of the dynamic differential pressure signal of Venturi meter for wet gas metering. *Flow Meas. Instrum.* Vol.14,No.4, pp.211-7, ISSN: 0955-5986

Zhang, F. S.; Dong, F. & Tan, C. (2010). High GVF and low pressure gas_liquid two-phase flow measurement based on dual-cone flowmeter. *Flow Meas. Instrumen.* Vol.21, No.3, pp. 410-417, ISSN: 0955-5986

Zheng, G. B.; Jin, N. D.; Jia, X. H. ; Lv, P. J. & Liu, X. B. (2008). Gas-liquid two phase flow measurement method based on combination instrument of turbine flowmeter and conductance sensor. *Int. J. of Multiphase Flow*, Vol.34, No.11, pp.1031-1047, ISSN: 0301-9322

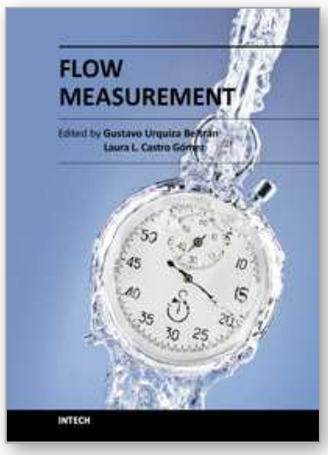

Flow Measurement

Edited by Dr. Gustavo Urquiza

ISBN 978-953-51-0390-5
Hard cover, 184 pages
Publisher InTech
Published online 28, March, 2012
Published in print edition March, 2012

The Flow Measurement book comprises different topics. The book is divided in four sections. The first section deals with the basic theories and application in microflows, including all the difficulties that such phenomenon implies. The second section includes topics related to the measurement of biphasic flows, such as separation of different phases to perform its individual measurement and other experimental methods. The third section deals with the development of various experiments and devices for gas flow, principally air and combustible gases. The last section presents 2 chapters on the theory and methods to perform flow measurements indirectly by means on pressure changes, applied on large and small flows.

InTech Europe
University Campus STeP Ri
Slavka Krautzeka 83/A
51000 Rijeka, Croatia
Phone: +385 (51) 770 447
Fax: +385 (51) 686 166
www.intechopen.com

InTech China
Unit 405, Office Block, Hotel Equatorial Shanghai
No.65, Yan An Road (West), Shanghai, 200040, China
中国上海市延安西路65号上海国际贵都大饭店办公楼405单元
Phone: +86-21-62489820
Fax: +86-21-62489821

IntechOpen